Experimental Tests of QCD

1. Test of QCD in e+e- annihilation
2. Running of the strong coupling constant
3. Study of QCD in deep inelastic scattering
4. Hadron-hadron collisions
5. Quark Gluon Plasma in Heavy Ion collisions

Discuss QCD tests in the following processes

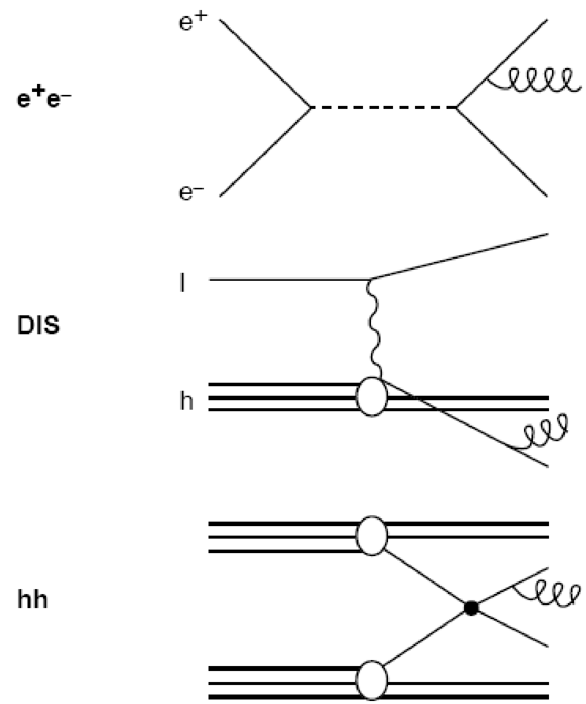

Historical Recap: Discovery of the Gluon and its Spin

$$e^+e^- \rightarrow q\bar{q}$$

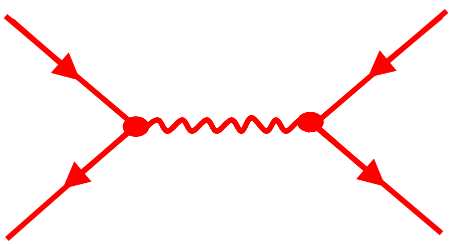

local parton
hadron duality

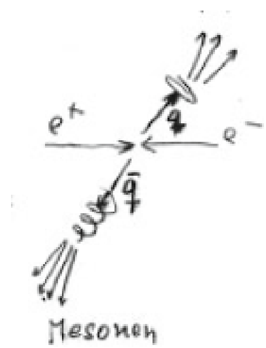

One of the first 2-jet events at PETRA

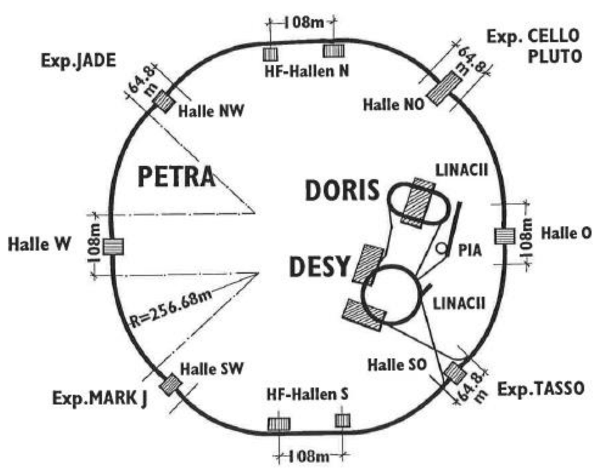

<u>Remark:</u>

PETRA (1978 -) was e^+e^- circular accelerator at DESY: operated at $\sqrt{s}$ between 13 and 46 GeV.

Earlier e^+e^- machines (e.g. SPEAR) with $\sqrt{s}_{max} \approx$ 10 GeV: ee→qq events have been observed, however events much less jet-like (more spherical) due to the smaller boost.

Quantify the 2-jet-likeness

$$T = \max \frac{\sum_i |\vec{p}_i \cdot \vec{n}_T|}{\sum_i |\vec{p}_i|}$$

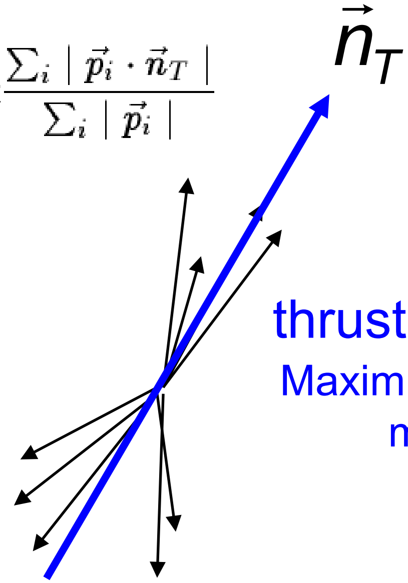

Expect T close to 1

Thrust distribution

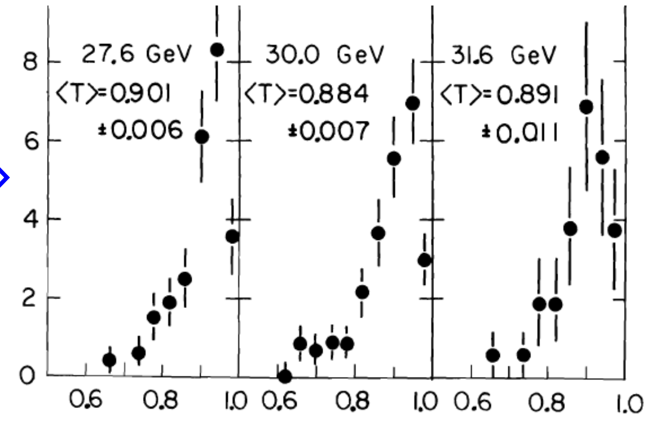

thrust axis = jet axis

Maximizes longitudinal momentum

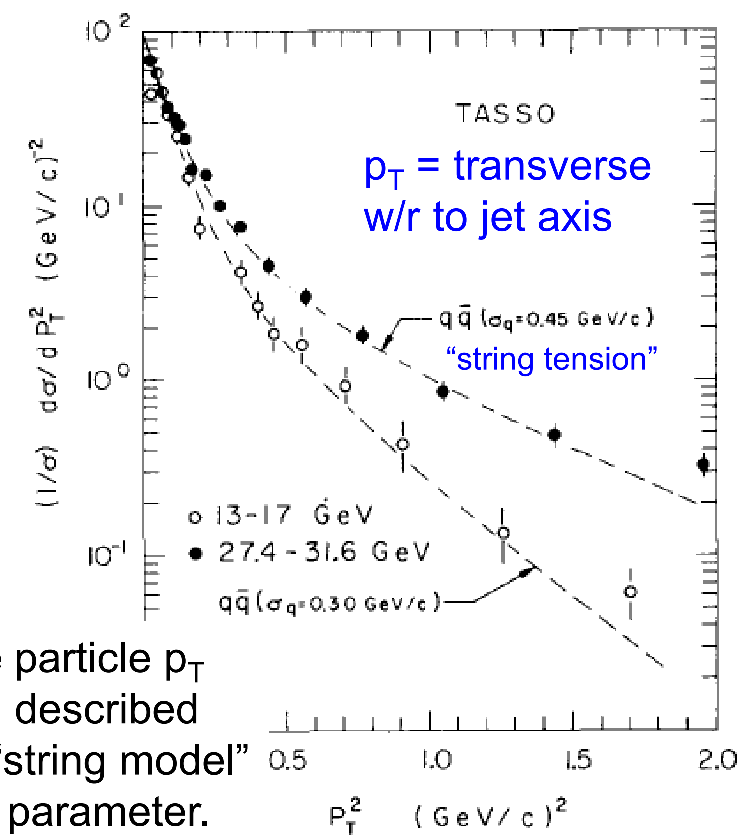

Thrust axis also defines the jet-axis

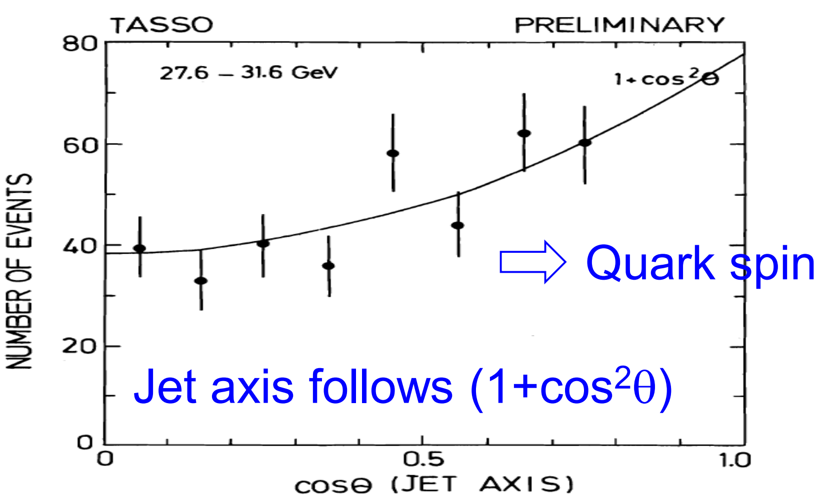

Also single particle p_T distribution described by simple "string model" with single parameter.

3-jet events:

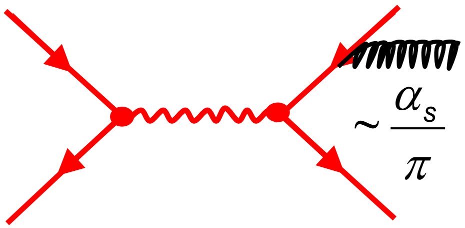

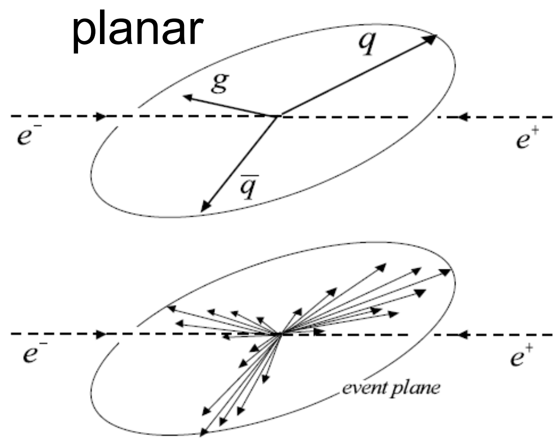

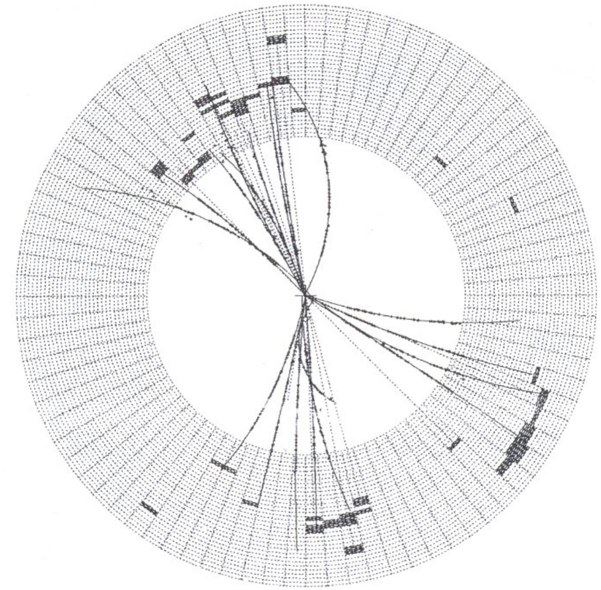

Fig. 11.12 A three-jet event observed by the JADE detector at PETRA.

But: How to exclude that the observed 3-jet signatures are fluctuations?

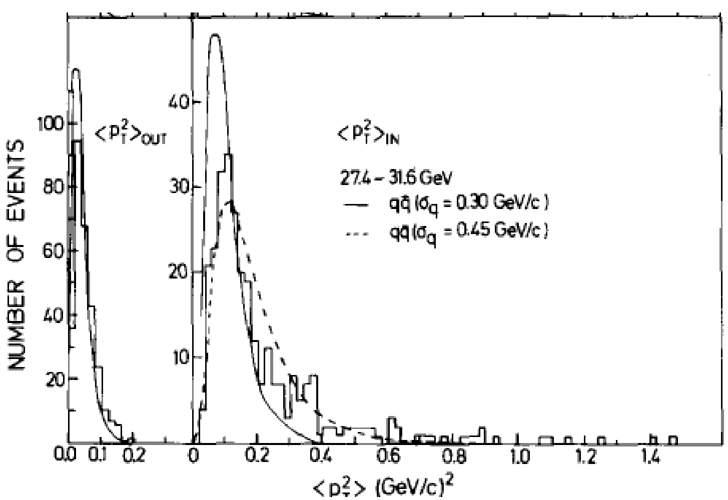

Check transverse $<p_T^2>$ outside and inside event plane: fluctuations should be the same: Outside $<p_T^2>$ well described by 2-jet model. Inside: "broadening" cannot be described, even not by higher string-tension.

Exp: $$\frac{\#3-\text{jet events}}{\#2-\text{jet events}} \approx 0.15 \sim \frac{\alpha_s}{\pi}$$

Spin of the Gluon:

Angular distribution of jets depend on gluon spin:

Ordering of 3 jets: $E_1 > E_2 > E_3$ Likely to be gluon

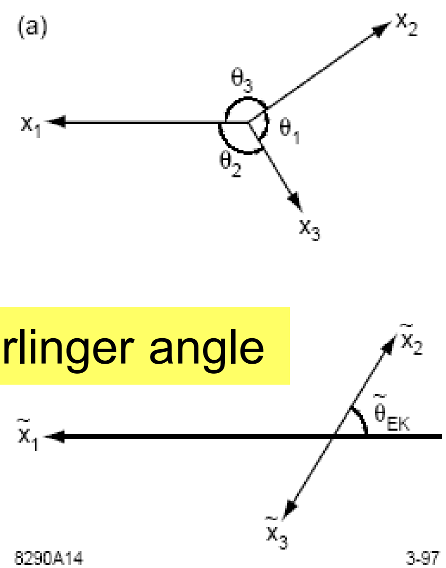

Ellis-Karlinger angle

Figure 8: (a) Representation of the momentum vectors in a three-jet event, an (b) definition of the Ellis-Karliner angle.

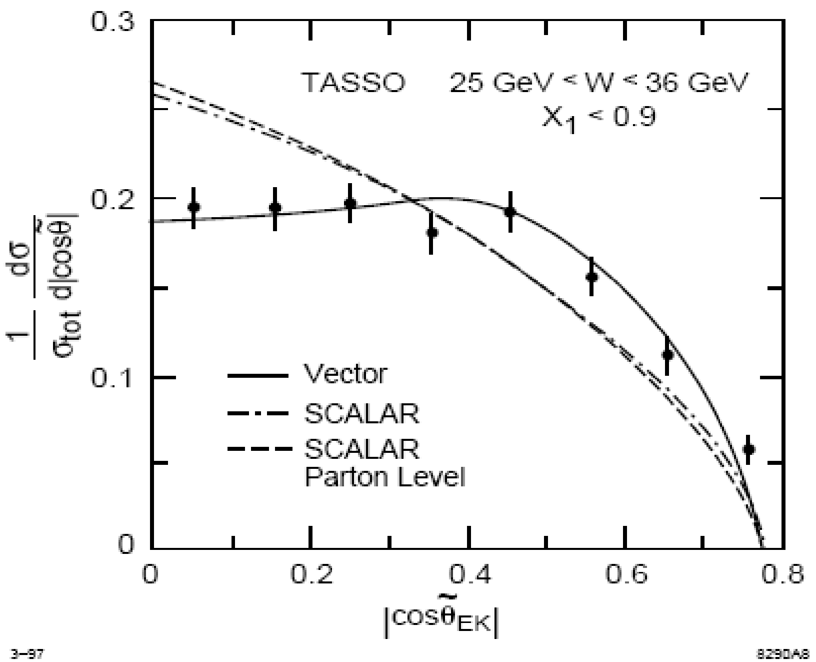

Figure 9: The Ellis-Karliner angle distribution of three-jet events recorded by TASSO at $Q \sim 30$ GeV [18]; the data favour spin-1 (vector) gluons.

Measure direction of jet-1 in the rest frame of jet-2 and jet-3: θ_{EK}

Gluon spin J=1

Theory Recap: Couplings and Color Factors

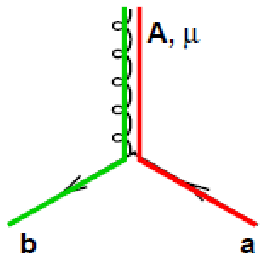

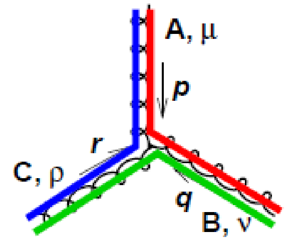

couplings

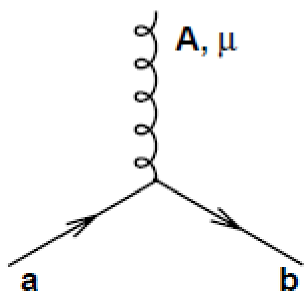

$$-ig_s t^A_{ba}\gamma^\mu$$

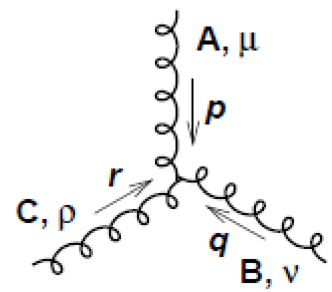

$$-g_s f^{ABC}[(p-q)^\rho g^{\mu\nu} \\ +(q-r)^\mu g^{\nu\rho} \\ +(r-p)^\nu g^{\rho\mu}]$$

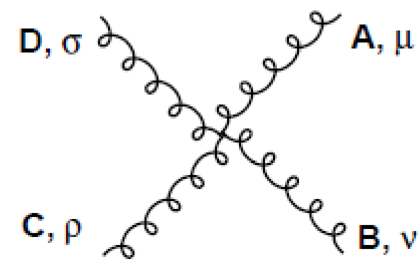

$$-ig_s^2 f^{XAC} f^{XBD}[g^{\mu\nu}g^{\rho\sigma} - g^{\mu\sigma}g^{\nu\gamma}] + \\ (C,\gamma)\leftrightarrow(D,\rho) + (B,\nu)\leftrightarrow(C,\gamma)$$

$|M|^2 \sim \alpha_s$

$|M|^2 \sim \alpha_s$

$|M|^2 \sim \alpha_s{}^2$

Color factor N_C for simple cross section

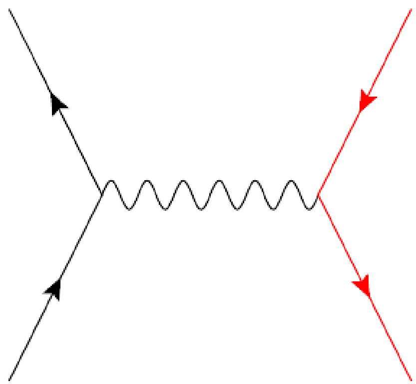

Hadronic Z decay

$e^- e^+ \to \gamma^*/Z^0 \to q\bar{q}$

$\propto N_C$

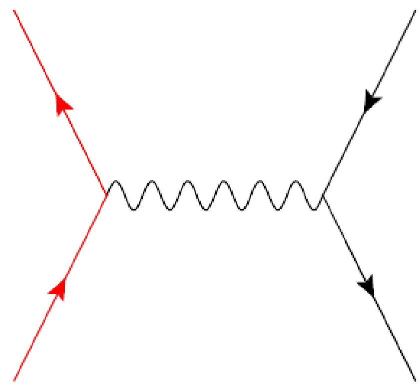

Drell-Yan

$q\bar{q} \to \gamma^*/Z^0 \to \ell^+\ell^-$

$\propto 1/N_C$

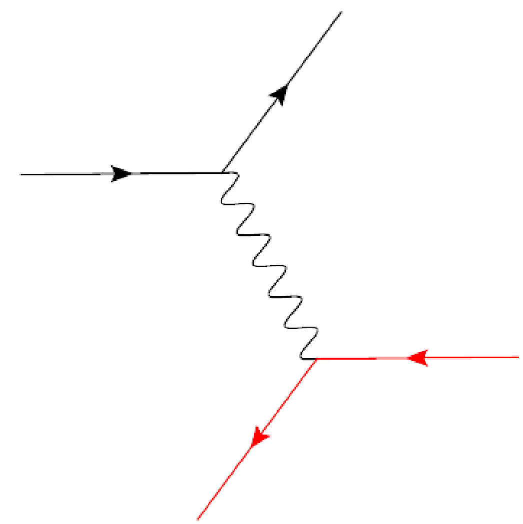

DIS

$\ell\bar{q} \xrightarrow{\gamma^*/Z^*} \ell\bar{q}$

$\propto 1$

Color factors

	Trace Relation	Indices	Occurs in Diagram Squared
(gluon splitting)^2	$\mathrm{Tr}\{t^a t^b\} = T_R\,\delta^{ab}$	$a, b \in [1, \ldots, 8]$	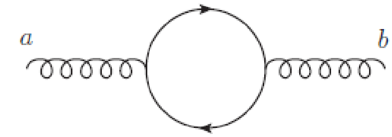
(quark color charge)^2	$\sum_a t^a_{ij} t^a_{jk} = C_F\,\delta_{ik}$	$a \in [1, \ldots, 8]$ $i, j, k \in [1, \ldots, 3]$	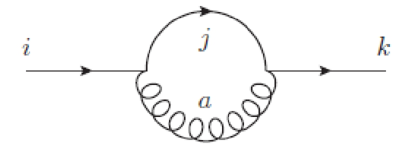
(Gluon color charge)^2	$\sum_{c,d} f^{acd} f^{bcd} = C_A\,\delta^{ab}$	$a, b, c, d \in [1, \ldots, 8]$	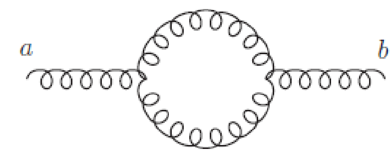

Example: $Z \to q g \bar{q}$:

$$\sum_{\text{colours}} |M|^2 \propto \delta_{ij} t^a_{jk} t^a_{k\ell} \delta_{\ell i}$$

$$= \mathrm{Tr}\{t^a t^a\}$$

$$= \frac{1}{2}\mathrm{Tr}\{\delta\} = 4\ ,$$

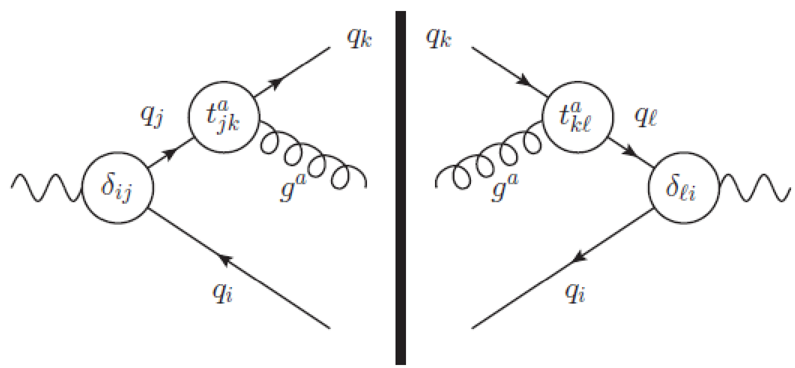

Casimirs of SU(3) in standard convention of generators

$$\boxed{T_R = \frac{1}{2} \qquad C_F = \frac{4}{3} \qquad C_A = N_C = 3\ .}$$

Test of QCD in e+e- annihilation

$$e^+e^- \rightarrow q\,\bar{q}$$

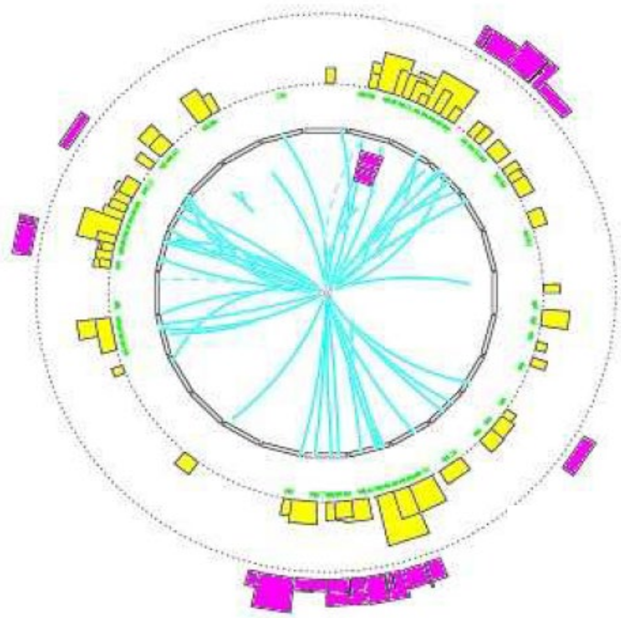

Theory Recap: Gluon radiation

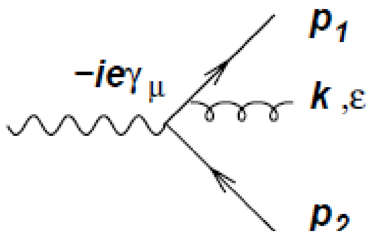

Gluon emission = infrared and collinear divergent

$$\sim \quad \frac{2\alpha_s C_F}{\pi} \frac{dE}{E} \frac{d\theta}{\sin\theta} \frac{d\phi}{2\pi}$$

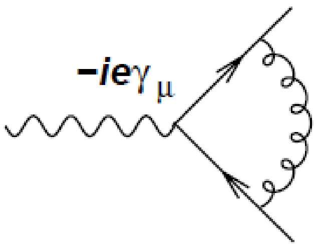

There are similar divergencies arising from the interference with loop diagrams – they cancel each other for small energy and small angles.

<u>Soft gluons don't matter for total cross section:</u>
Time scale for gluon emission ~1/Eθ much longer than hard process.
Hadronization w/ time scale ~1/Λ can also not influence "hard" process

Correction to the cross section (e.g. ee$\rightarrow$qq(g)) from large energy gluons.

$$\sigma_{tot} = \sigma_{q\bar{q}} \left(1 + 1.045 \frac{\alpha_s(Q)}{\pi} + 0.94 \left(\frac{\alpha_s(Q)}{\pi} \right)^2 - 15 \left(\frac{\alpha_s(Q)}{\pi} \right)^3 + \cdots \right)$$

"good" perturbativ e behavior

(coefficients determined at Z pole)

Soft collinear gluon emission – jet substructure

Integrate emission probability to get the mean number of gluons with $E_T \approx E\Theta > Q_0$ cut-off scale emitted off a quark with energy $Q >> Q_0$:

$$\langle N_g \rangle \simeq \frac{2\alpha_s C_F}{\pi} \int^{Q} \frac{dE}{E} \int^{\pi/2} \frac{d\theta}{\theta} \, \Theta(E\theta > Q_0)$$

$$\langle N_g \rangle \simeq \frac{\alpha_s C_F}{\pi} \ln^2 \frac{Q}{\Lambda_{QCD}}$$ for cut-off scale $Q_0 \approx \Lambda_{QCD}$:

$$\longrightarrow \langle N_g \rangle \simeq 2.2$$ for quark energies $Q \approx 100$ GeV

Surprisingly large for a perturbative result!

We need to consider next-orders.

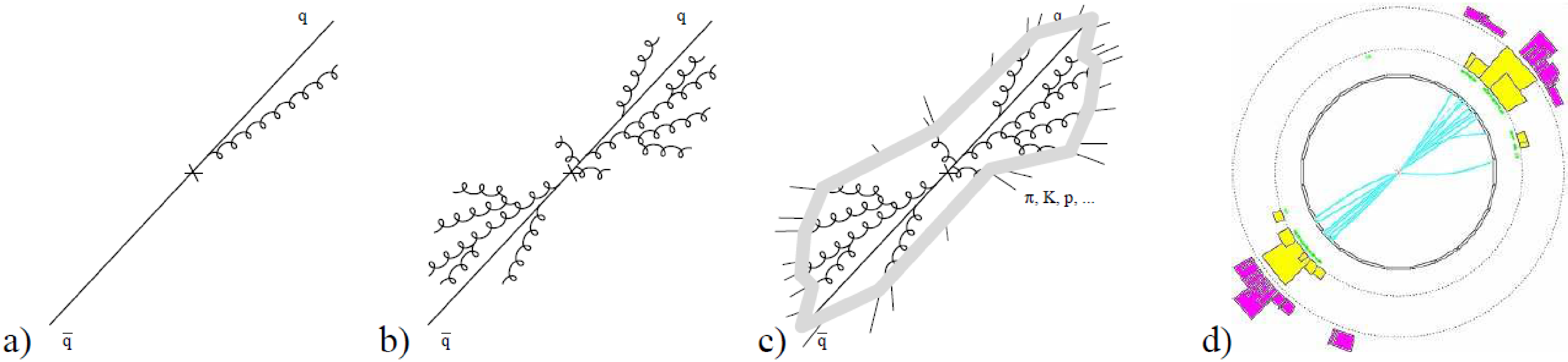

Possible to calculate the gluon multiplicity analytically, by summing all orders (n) of perturbation theory:

$$\langle N_g \rangle \sim \sum_n \frac{1}{(n!)^2} \left(\frac{C_A}{\pi b} \ln \frac{Q}{\Lambda} \right)^n$$

$$\sim \exp \sqrt{\frac{4 C_A}{\pi b} \ln \frac{Q}{\Lambda}}$$

Compare to hadron multiplicity in ee →hadrons (fit: overall normalization is free parameter):

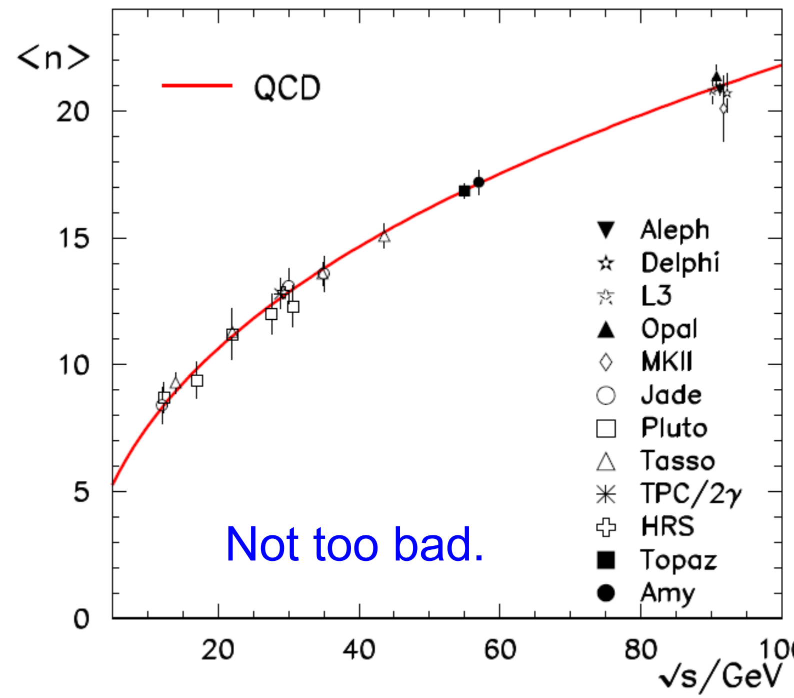

In general analytical calculation difficult: Instead use parton-shower Monte Carlos.

Simulation of hadronic final states:

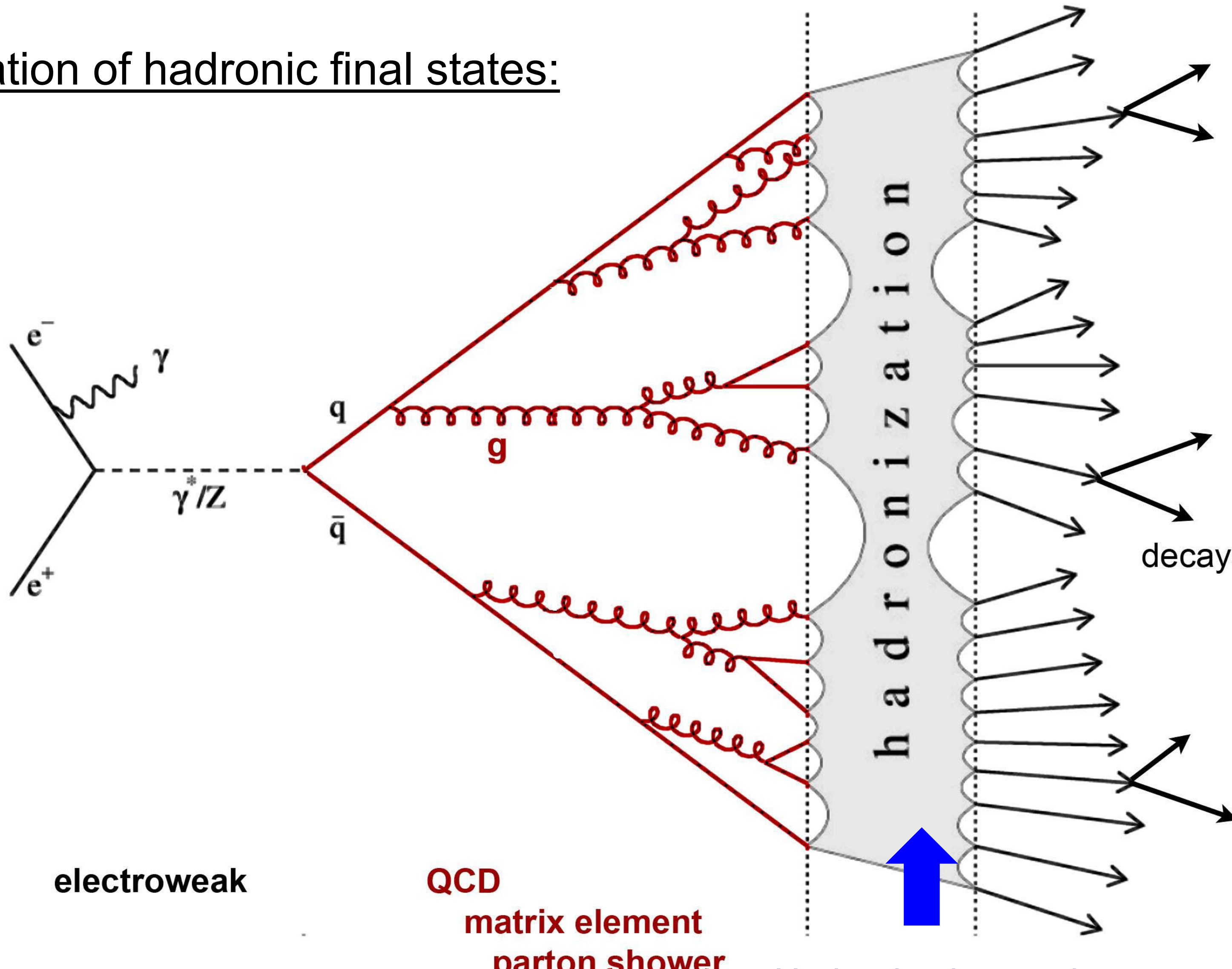

Tricky: “Matching”

Hadronization models:
String (JETSET) and cluster (HERWIG) fragmentation.

Infrared collinear safe (IRCS) observables

An observable is infrared and collinear safe if, in the limit of a collinear splitting, or the emission of an infinitely soft particle, the observable remains unchanged.

e.g; Thrust is IRCS

$$T = \max \frac{\sum_i |\vec{p}_i \cdot \vec{n}_T|}{\sum_i |\vec{p}_i|}$$

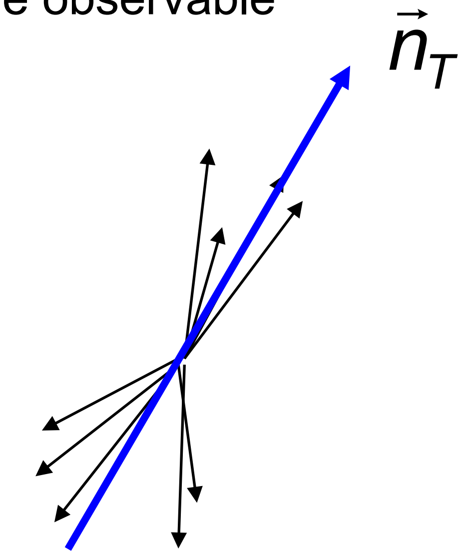

<u>Jets and jet algorithms are not necessary IRCS</u>

e.g. simple cone algorithms

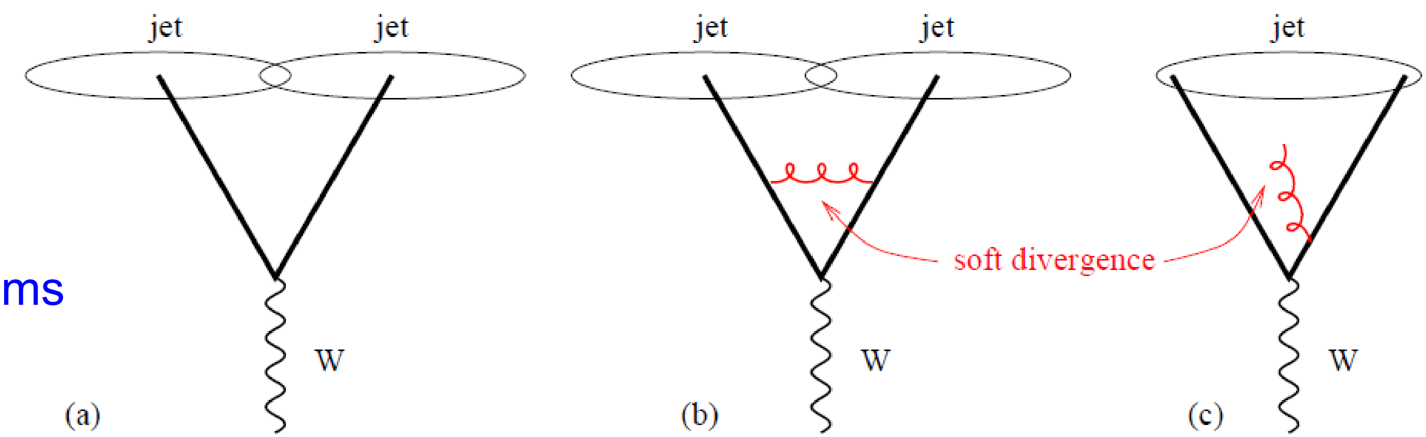

How many jets – jet algorithms?

Multi-jet event from OPAL

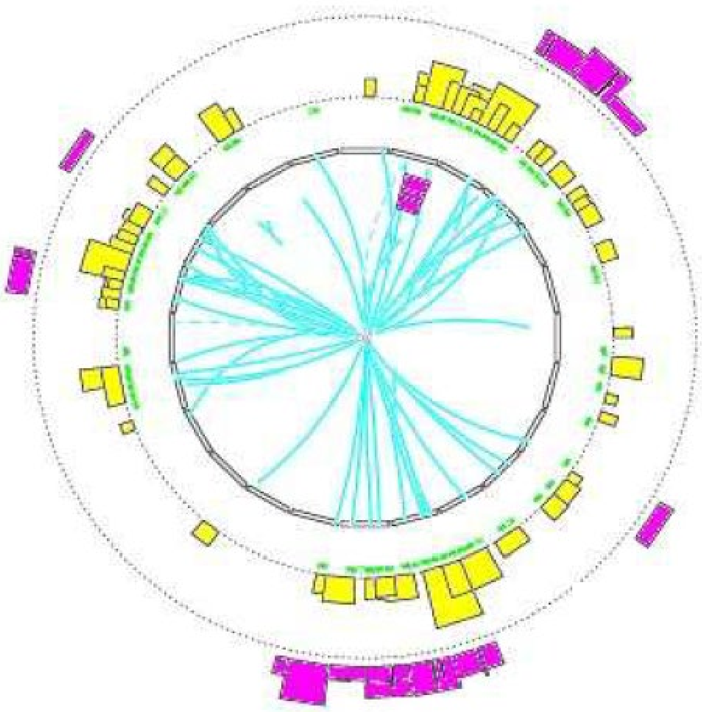

Problem:

There is no "natural" definition of jets.

Need well defined algorithms which are also applicable to "theoretical calculations", i.e. at parton level.

In addition jet-algorithms should be "collinear" and "infra-red" safe:

Jet Algorithms

Iterative Jet algorithms ("Jade"-type, developed for $e^+ e^-$)

1) for all pairs of particles i, j calculate distance parameter y_{ij}

2) find pair i, j with smallest $y_{ij,\,\mathrm{min}}$

3) add 4-momenta: $p_i + p_j = p_k$ replace p_i, p_j by p_k

4) iterate till $y_{ij} > y_{\mathrm{cut}}$

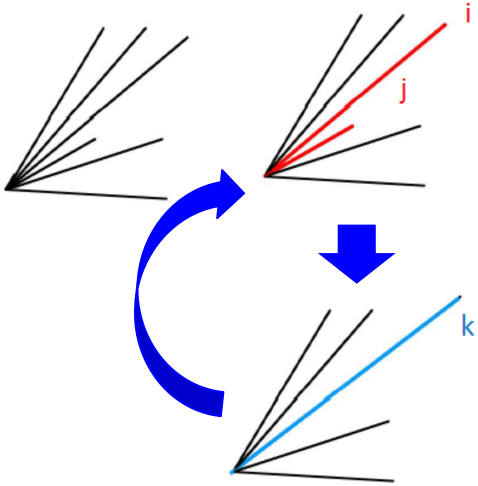

Distance measures:

$$y_{ij} = 2\,\frac{E_i\,E_j\,(1-\cos\theta_{ij})}{s}$$

$$y_{ij} = 2\,\frac{\min(E_i^{\,2},E_j^{\,2})(1-\cos\theta_{ij})}{s}$$

$$\min(E_i^2,E_j^2) \to \min(E_i^{-2},E_j^{-2})$$

Jade algorithm: IRCS but theoretically difficult; large higher order correction.
(invariant mass squared)

k_T – algorithm:
better higher order behavior
(relative transverse momentum squared)

anti-k_T – algorithm: often used nowadays
(→jets with only soft radiation are conical)

Adaptation for hadron colliders

Due to kinematics the "jet cone" at hadron collider needs an adapted definition:

Use rapidity $y_i = \frac{1}{2}\ln\frac{E_i + p_{z,i}}{E_i - p_{z,i}}$ and azimuthal angle ϕ_i:

Often use pseudo rapidity η

$$\eta = -\ln\left(\tan\frac{\theta}{2}\right)$$

→ angular distance of 2 particles: $\Delta R_{ij}^{\;2} = (y_i - y_j)^2 - (\phi_i - \phi_j)^2$

(anti)-k_t algorithm:

$$\boxed{d_{ij} = \min(p_{t,i}^{2l-2}, p_{t,i}^{2l-2}) \cdot \frac{\Delta R_{ij}^{\;2}}{R^2}}$$

Parameter to describe typ. jet opening: R=0.4…0.7 (see below)

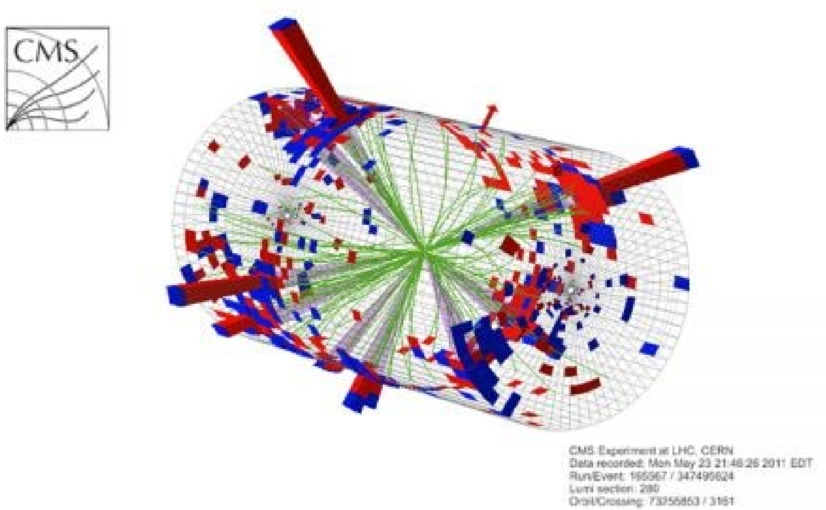

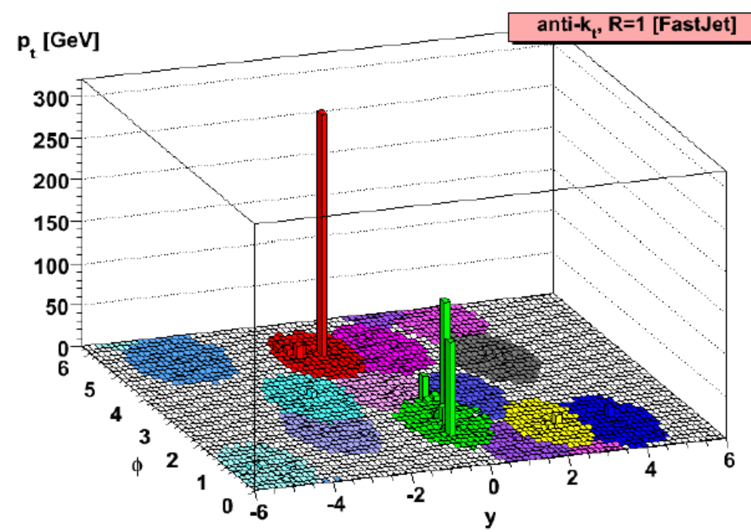

Cone algorithms

Simplest cone algorithm: Iterative cone algorithms w/ progressive removal

1) Order particles according transverse momentum
2) Select particle i w/ largest pt as seed particle
3) Draw a cone with radius R (see above) around i:
   consider all particles j with ΔR_{ij} < R w/r to i and calculate the sum of the momenta $\vec{P}$
4) Check with seed direction – if it does not coincide, chose $\vec{P}$ as new seed and repeat procedure.
5) If stable cone found: remove all particles from the list.

Easy procedure, but not infrared safe (if seed particle loses energy…) – true for many other cone algorithms as well.

There are Seedless Infrared Safe Cone Algorithms (SISCone) to overcome the problem.

Cone algo: “nice jets”

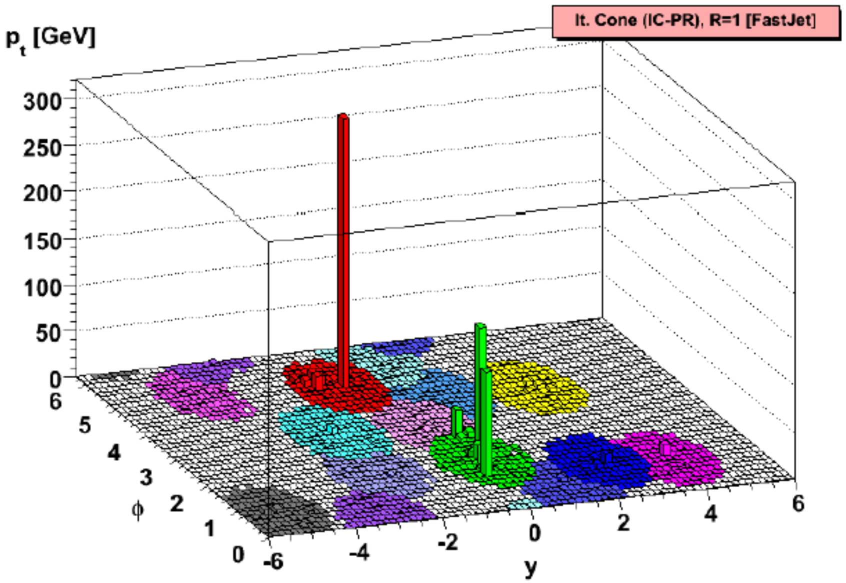

kt algo: “fuzzy jets”

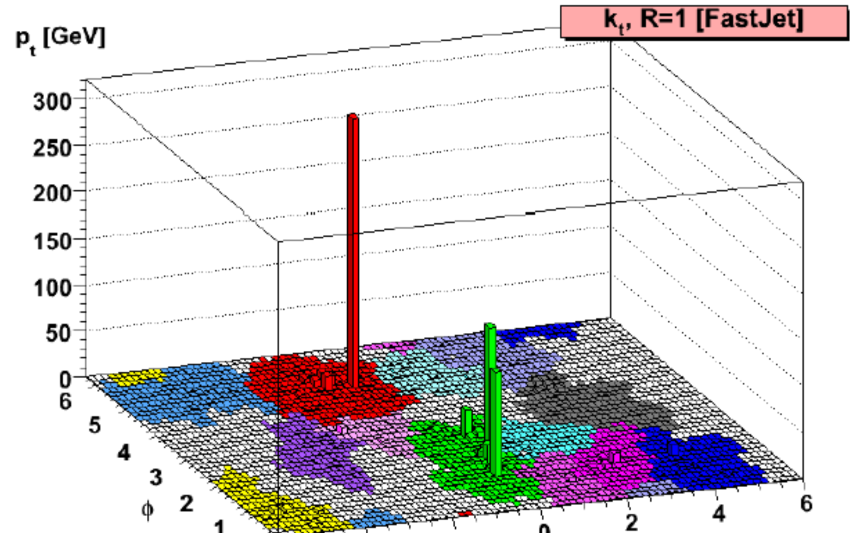

Anti-kt: “nice jets”

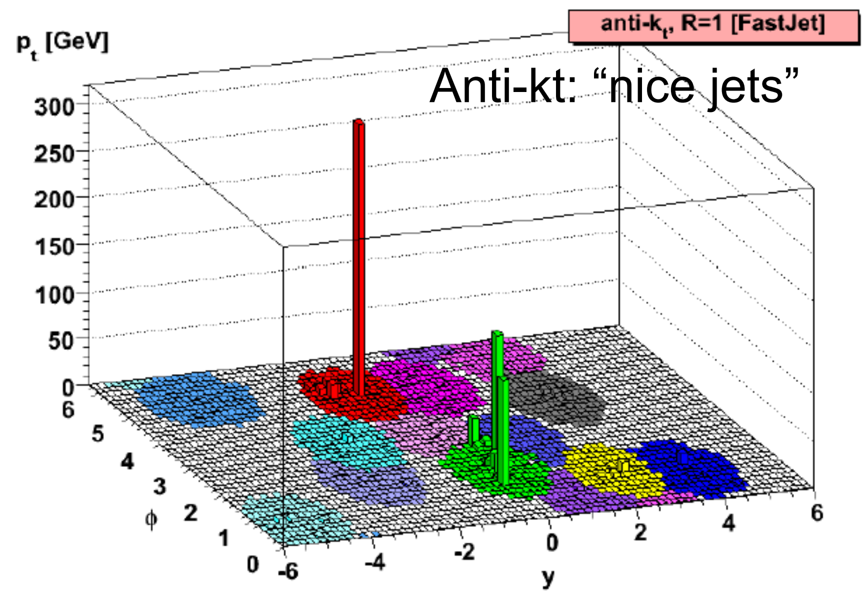

“The” jet algorithm does not exist – depends on what you want to do.

Meanwhile the most common algorithm is the anti-kt algorithm (fast, IRCS, nice jets)

Multiple-jet events in e^+e^- annihilations: ee → hadrons @ $\sqrt{s}\approx 91$ GeV

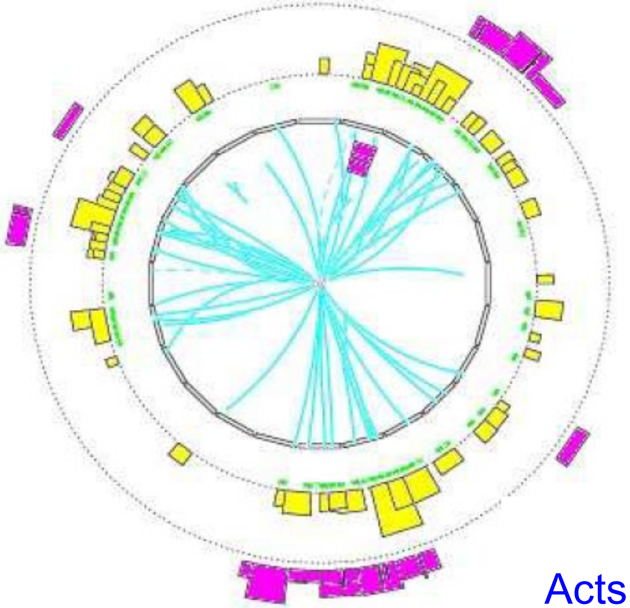

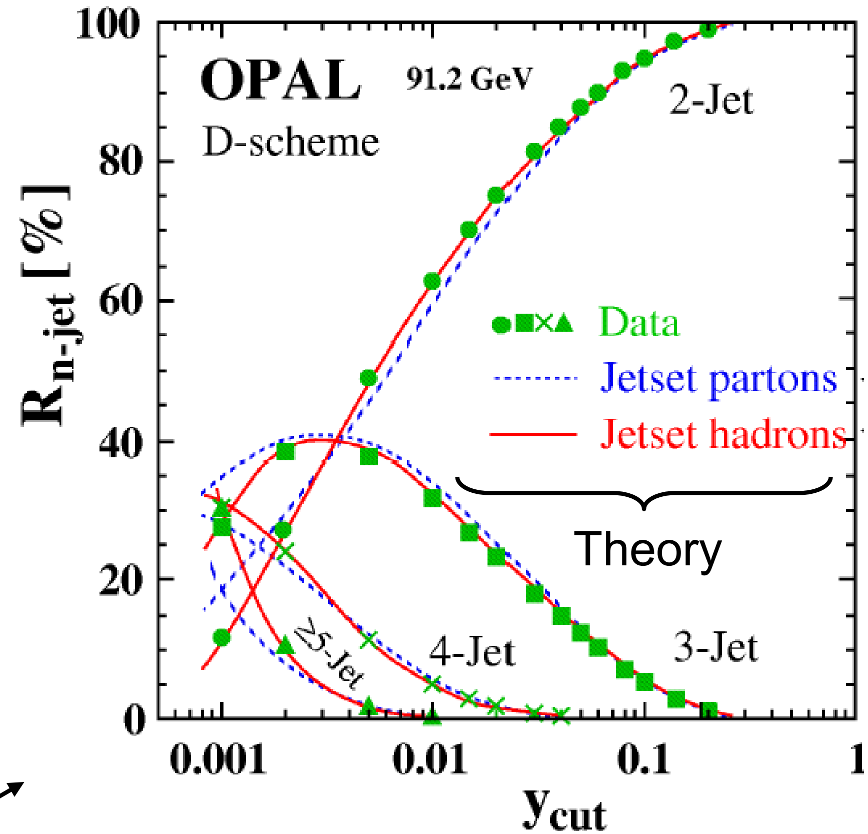

Acts as resolution parameter

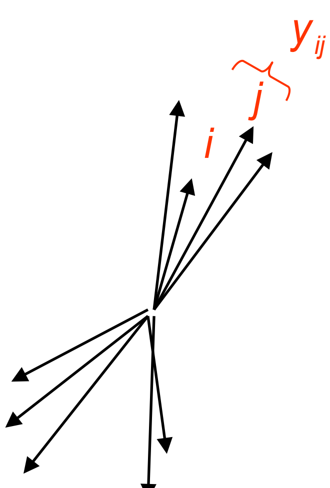

$y_{ij} \geq y_{cut}$

Exclusive n-jet cross section:

$$\sigma_{3-jet} = c_0 \frac{\alpha_s}{\pi}(1 + c_1 \frac{\alpha_s}{\pi} + ...) \cdot \sigma_{qq}$$

$$\sigma_{4-jet} = c_0' \frac{\alpha_s^2}{\pi}(1 + c_1' \frac{\alpha_s}{\pi} + ...) \cdot \sigma_{qq}$$

⇨ Determination of α_s

4-jet events: Gluon self coupling and color factors

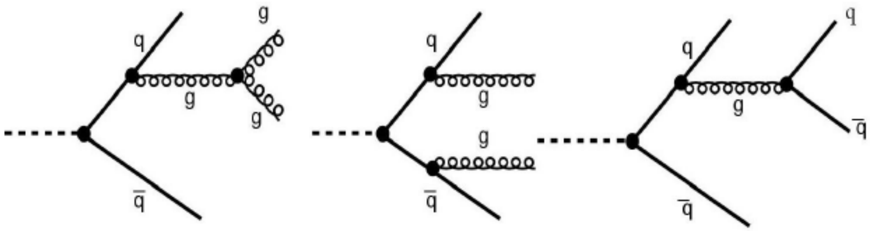

L3 Coll., Phys. Lett. B248 (1990)

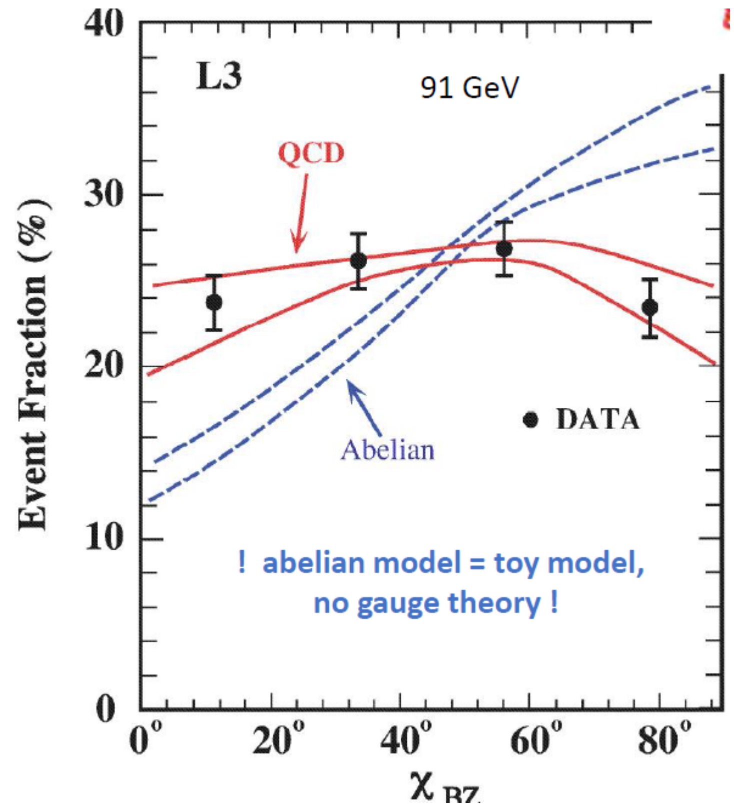

4-jet observable that is sensitive to the ratios of Casimir factors: Bengtsson-Zerwas angle

Order and labels the four jets in an event in terms of their momenta (or energies) such that p1 > p2 > p3 > p4 can define the Bengtsson-Zerwas angle: jet3 and jet4 probable gluon jets.

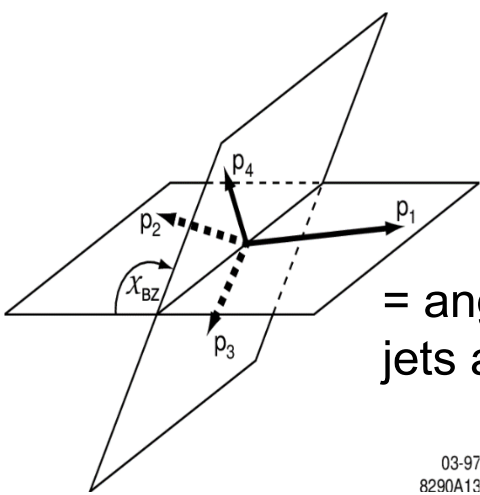

= angle between plane w/ 2 leading jets and plane w/ 2 non-leading jets.

4-jet cross section

$$\sigma \sim C_F \cdot \sigma_A + (C_F - C_A/2) \cdot \sigma_B$$

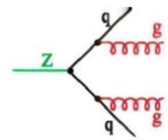

qqgg

$$+ \boxed{C_A} \cdot \sigma_C$$

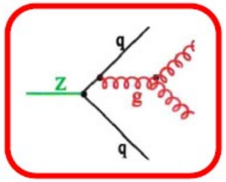

$$+ T_R \cdot \sigma_D + (C_F - C_A/2) \cdot \sigma_E$$

qqqq

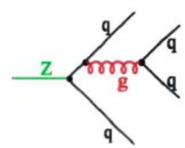

$$d\sigma^{(4)} \propto \left(\frac{\alpha_s C_F}{\pi}\right)^2 \left[A(y_{ij}) + \left(1 - \frac{1}{2}\frac{C_A}{C_F}\right) B(y_{ij}) + \left(\frac{C_A}{C_F}\right) C(y_{ij}) + \left(n_f \frac{T_R}{C_F}\right) D(y_{ij}) + \left(1 - \frac{1}{2}\frac{C_A}{C_F}\right) E(y_{ij}) \right],$$

A,B,C,D,E= angular dependent kinematic functions.

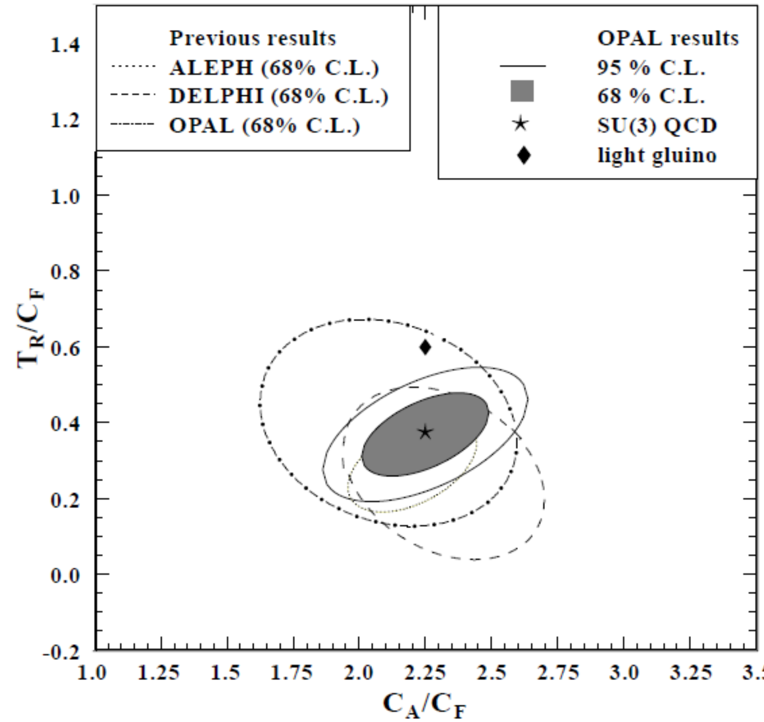

$$\alpha_s = 0.120 \pm 0.011(\text{stat.}) \pm 0.020(\text{syst.})$$
$$C_A = 3.02 \pm 0.25(\text{stat.}) \pm 0.49(\text{syst.})$$
$$C_F = 1.34 \pm 0.13(\text{stat.}) \pm 0.22(\text{syst.})$$

(w T_R =1/2)

QCD (SU(3)): C_F=4/3 C_A=3

2. "Running" of the strong coupling α_s

Recap:

Propagator corrections:

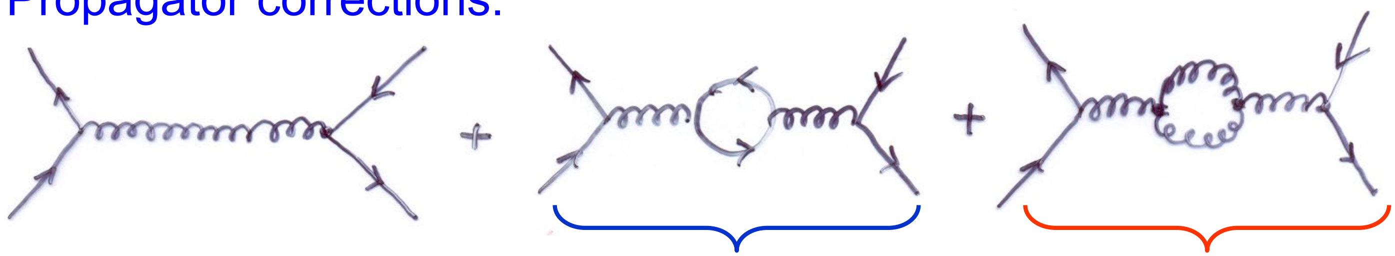

"screening" "anti-screening"

Strong coupling $\alpha_s(Q^2)$

$$\boxed{\alpha_s(Q^2) = \frac{\alpha_s(\mu^2)}{1 + \alpha_s(\mu^2)\beta_0 \log\frac{Q^2}{\mu^2}}}$$

$$\beta_0 = \frac{1}{12\pi}(33 - 2n_f)$$

n_f = active quark flavors

μ^2 = renormalization scale

conventionally $\mu^2 = M_Z^2$

$$\alpha_s(Q^2) = \frac{1}{\beta_0 \log(Q^2/\Lambda_{QCD}^2)}$$

with $\Lambda_{QCD} \approx 210\,\mathrm{MeV}$

scale at which perturbation theory diverges

Measurement of Q^2 dependence of α_s

➡ α_s measurements are done at given scale Q^2: $\alpha_s(Q^2)$

a) α_s from total hadronic cross section at Z pole

$$e^+e^- \to q\,\bar{q}(g)$$

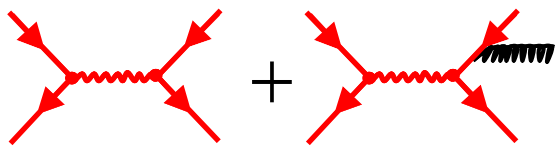

Final state gluon radiation.

$$\sigma_{had}(s) = \sigma_{had}^{QED}(s)\left[\underbrace{1 + 1.05 \cdot \frac{\alpha_s(s)}{\pi} + 0.9 \cdot \frac{\alpha_s(s)^2}{\pi^2} + \ldots}_{1+\delta_{QCD}}\right]$$

$$R_{had} = \frac{\sigma(ee \to hadrons)}{\sigma(ee \to \mu\mu)} = 3\sum Q_q^2 \left[1 + 1.05 \cdot \frac{\alpha_s(s)}{\pi} + 0.9 \cdot \frac{\alpha_s(s)^2}{\pi^2} + \ldots\right]$$

Example:

$$R_{had}^Z = 20.89 \pm 0.13$$

$$\delta_{QCD} = 0.0461 \pm 0.0065$$

$$\alpha_s(m_z) = 0.136 \pm 0.019$$

b) α_s from hadronic event shape variables

3-jet rate: $R_3 \equiv \dfrac{\sigma_{3-jet}}{\sigma_{had}}$ depends on α_s

3-jet rate is measured as function of y_{cut}

QCD calculation provides a theoretical prediction for $R_3^{theo}(\alpha_s\ ,\ y_{cut})$

$\rightarrow$ fit $R_3^{theo}(\alpha_s\ ,\ y_{cut})$ to the data to determine α_s

Other event shape variables (sphericity, thrust,…) can be used to obtain a prediction for α_s

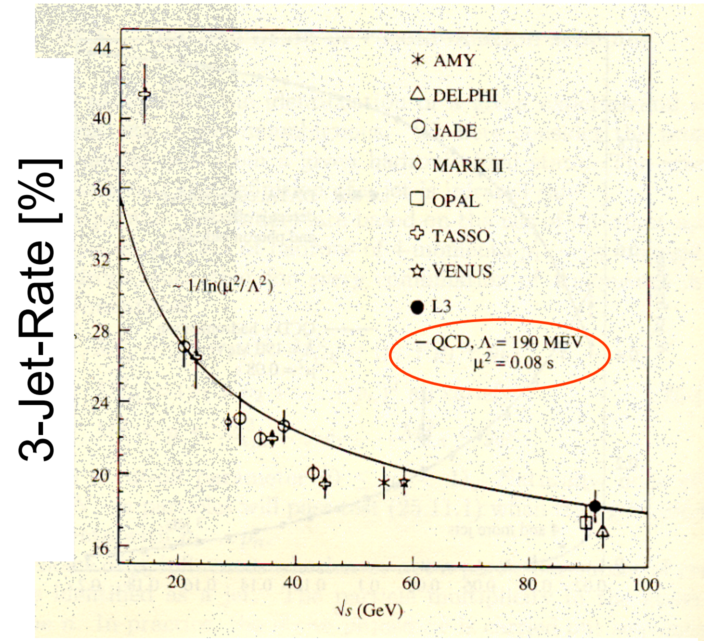

$$T = \max \frac{\sum_i |\vec{p}_i \cdot \vec{n}_T|}{\sum_i |\vec{p}_i|}$$

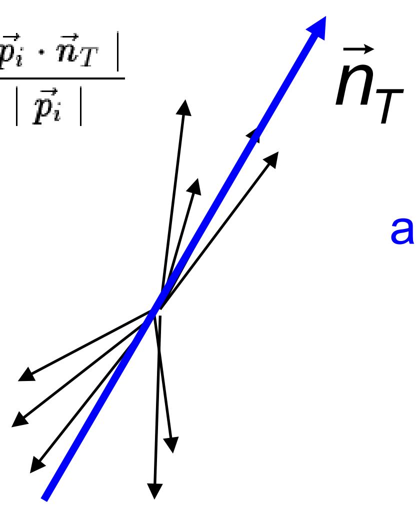

also function of α_s

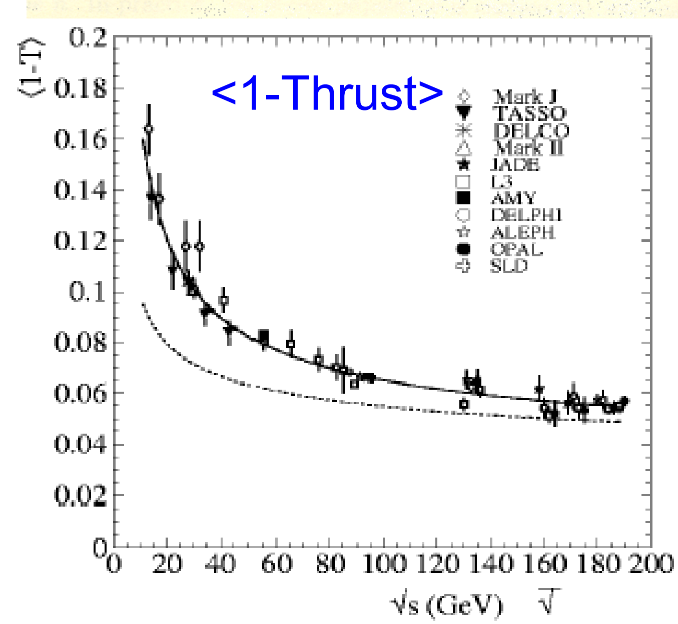

c) α_s from hadronic τ decays

$$R^{\tau}_{had} = \frac{\Gamma(\tau \to \nu_\tau + Hadrons)}{\Gamma(\tau \to \nu_\tau + e\overline{\upsilon}_e)} \sim f(\alpha_s)$$

$R^{\tau}_{had} =$

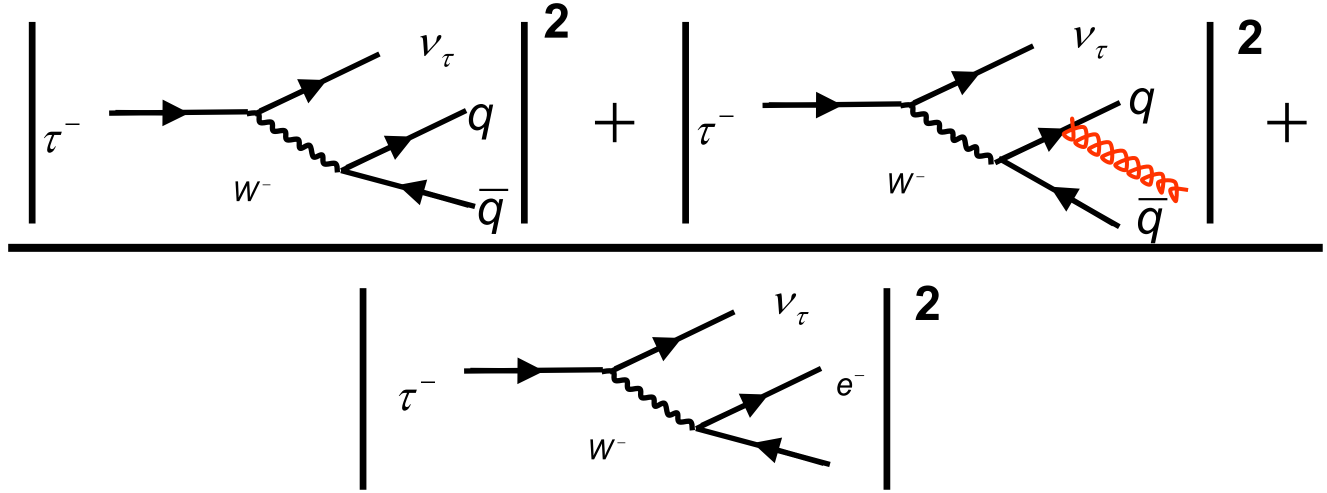

$$R^{\tau}_{had} = R^{\tau,0}_{had}\left(1 + \frac{\alpha_s(m_\tau^2)}{\pi} + \ldots\right)$$

d) α_s from DIS (deep inelastic scattering): DGLAP fits to PDFs

e) α_s from number of jets in pp (see sect. 3)

Running of α_s and asymptotic freedom

Experimental determination.

$$\alpha_s(M_Z^2) = 0.1175 \pm 0.0010$$

Alphas from the lattice:

$$\alpha_s(M_Z^2) = 0.1182 \pm 0.0008$$

Unweighted average w/ average uncertainty of the two:

$$\alpha_s(M_Z^2) = 0.1179 \pm 0.0009$$

Particle Data Group 2021

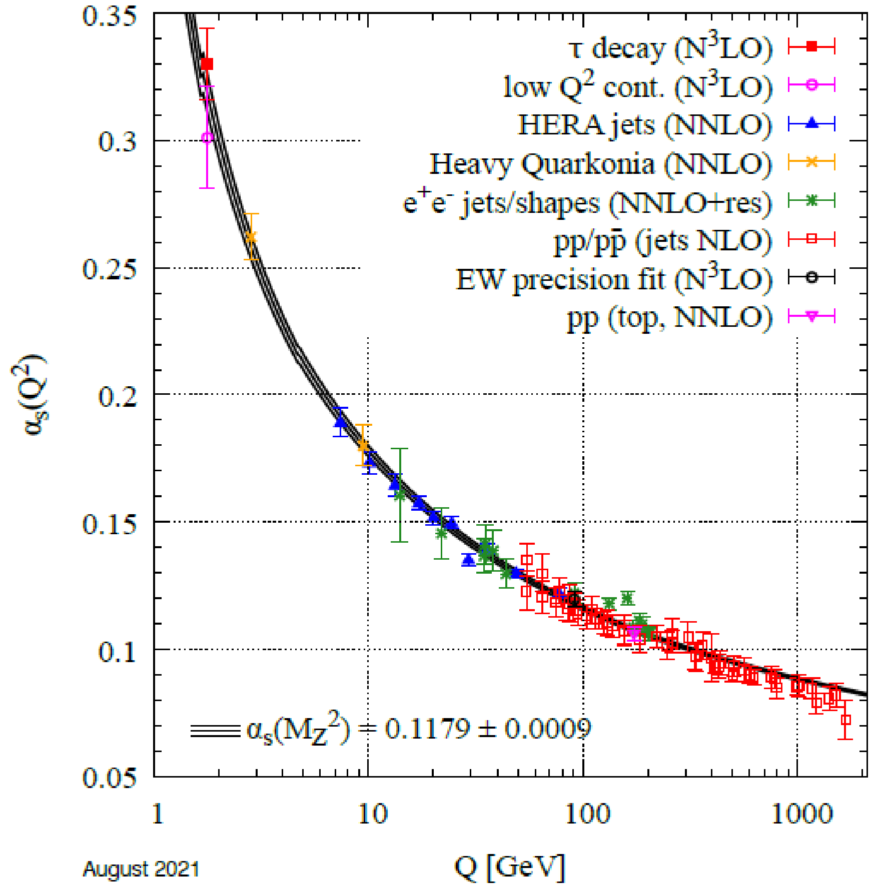

Figure 9.3: Summary of measurements of α_s as a function of the energy scale Q. The respective degree of QCD perturbation theory used in the extraction of α_s is indicated in brackets (NLO: next-to-leading order; NNLO: next-to-next-to-leading order; NNLO+res.: NNLO matched to a resummed calculation; N^{3}LO: next-to-NNLO).

3. Study of QCD in deep inelastic scattering (DIS)

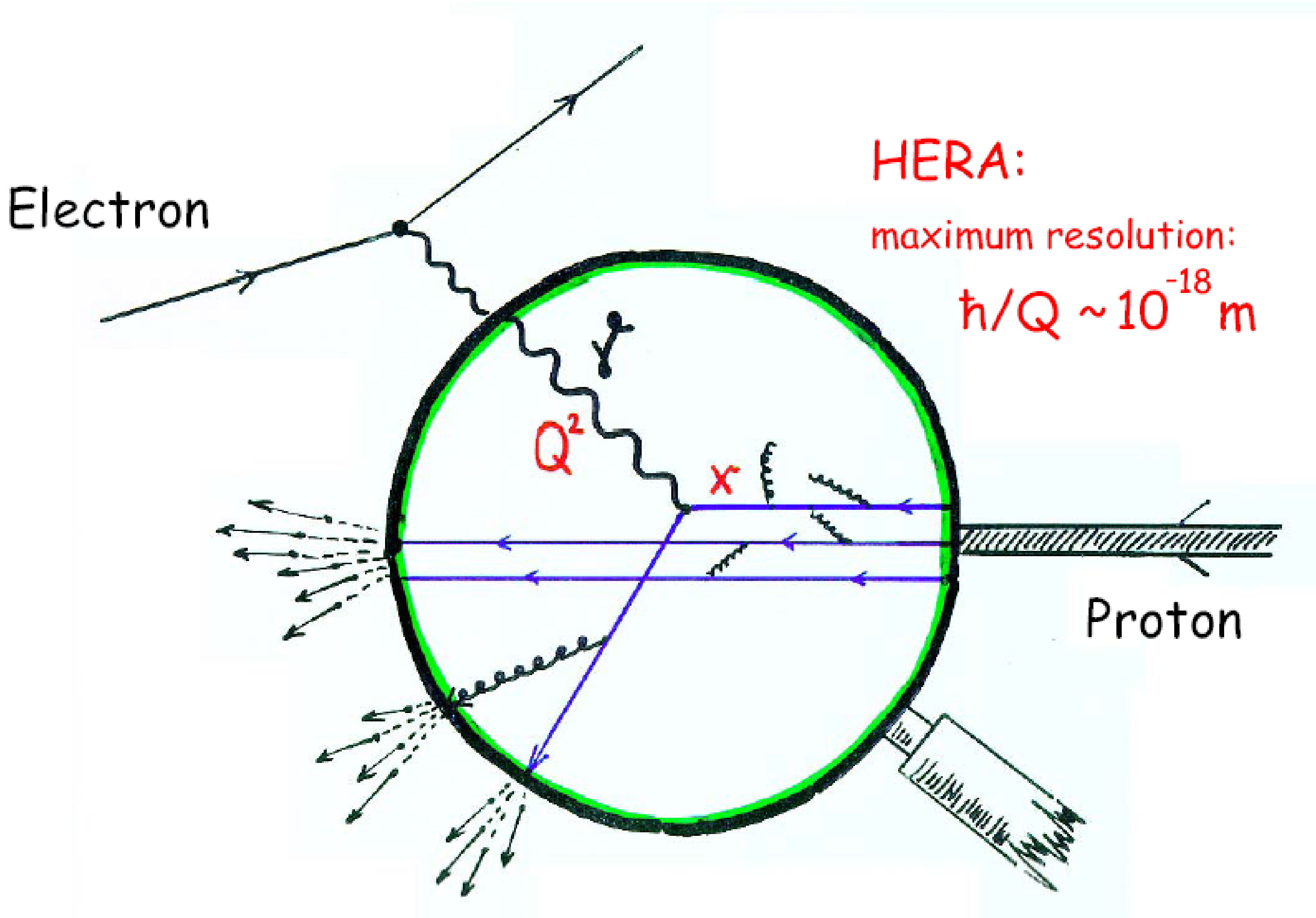

Courtesy: H.C. Schultz-Coulon

Recap: Deep-inelastic scattering - kinematics

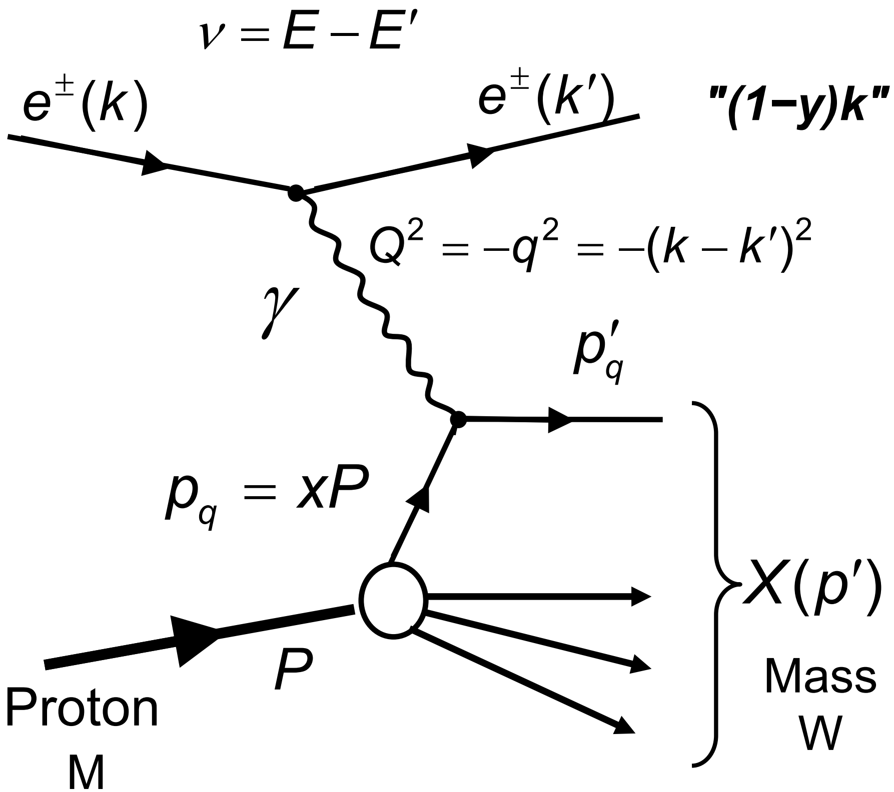

x = fractional momentum of struck quark

y = Pq/Pk = elasticity, fractional energy transfer in proton rest frame

ν = E - E′ = energy transfer in lab

$$y = \frac{P\cdot q}{P\cdot k}$$

fixed target

$$x = \frac{Q^2}{2P\cdot q} = \frac{Q^2}{2M\nu}$$ (Bjorken x)

$$Q^2 = sxy$$ s = CMS energy

Cross section in parton model (QPM)

σ 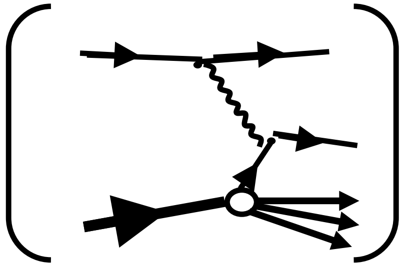 $= \sum_i q_i(x)\,\sigma_i$ 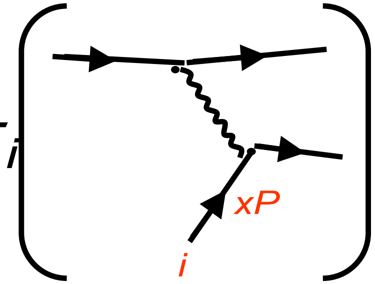

Parton density $q_i(x)dx$: Probability to find parton i in momentum interval [x, x+dx]

$$\frac{d^2\sigma}{dQ^2dx} = \left(\frac{4\pi\alpha^2}{Q^4}\right)\frac{E'}{E}\cdot \underbrace{\sum_i \int_0^1 e_i^2 \cdot q_i(\xi)\cdot\delta(x-\xi)d\xi}\left(\cos^2\frac{\theta}{2} + \frac{Q^2}{2x^2M^2}\sin^2\frac{\theta}{2}\right)$$

Parton distribution function PDF:

$$F_2(x) = x\sum_i \int_0^1 e_i^2 q_i(\xi)\cdot\delta(x-\xi)d\xi = x\sum_i e_i^2 q_i(x)$$

$$F_1(x) = \frac{1}{2}\sum_i e_i^2 q_i(x)$$

$F_2 = F_2\,(x)$

Photon exchange $\sim e_i^2$ does not distinguish between quark and anti-quarks.

$$\frac{d^2\sigma}{dQ^2dx} = \left(\frac{4\pi\alpha^2}{Q^4}\right)\frac{E'}{E}\cdot\left(\frac{F_2(x)}{x}\cos^2\frac{\theta}{2} + 2F_1(x)\frac{Q^2}{2x^2M^2}\sin^2\frac{\theta}{2}\right)$$

Kinematical relations

$$\frac{d^2\sigma}{dQ^2dx} = \left(\frac{4\pi\alpha^2}{xQ^4}\right)\cdot\left((1-y)F_2(x) + xy^2F_1(x)\right)$$

Deep inelastic electron-proton scattering:

- Free partons: $F_2=F_2(x)$ $\Leftrightarrow$ "scaling" (F_2 only function of x)
- Spin ½ partons: $2xF_1(x) = F_2(x)$ (Callan-Gross relation)

$$\frac{d^2\sigma}{dQ^2dx} = \left(\frac{4\pi\alpha^2}{xQ^4}\right)\cdot\left(\frac{1+(1-y)^2}{2}F_2(x) \quad + \mathcal{O}(\alpha_s)\right)$$

Parton level, i.e. ignoring QCD corrections

Scaling & scaling violation (early measurements)

Region of 1st SLAC measurement (1972):

Scaling: $F_2 = F_2(x)$, PDFs are independent of Q^2 (QPM).

For larger Q^2 and diff. x:

$$F_2 = F_2(x, Q^2) = x \sum_i e_i^2 q_i(x)$$

PDFs are functions of Q^2 as expected when considering QCD correction.

μ scattering

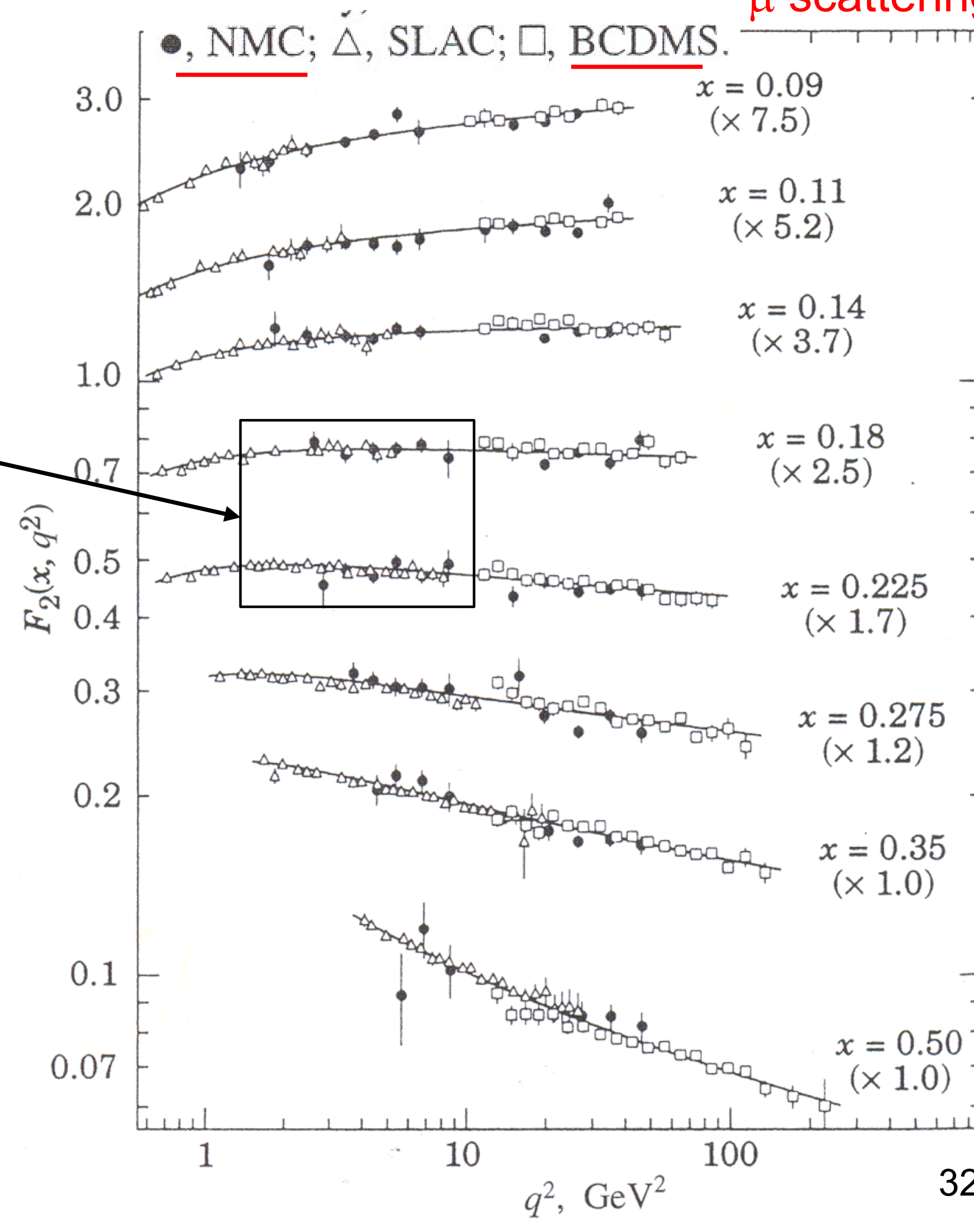

Experimental determination of quark and gluon distributions

Scattering at isoscalar target N with #n=#p and assuming isospin symmetry:

Isoscalar Target: #n=#p

$$F_2^N = \frac{1}{2}\left[F_2^p + F_2^n\right] = \frac{5}{18}x \cdot [u + \bar{u} + d + \bar{d}] + \frac{1}{9}x \cdot [s + \bar{s}]$$

Use neutrino (anti-neutrino) scattering (w/ W exchange) to distinguish between quark and anti-quark and to extract experimentally valence and sea quark distributions ($\rightarrow$ new structure functions F_3 to account parity violation).
For iso-scalar target one finds:

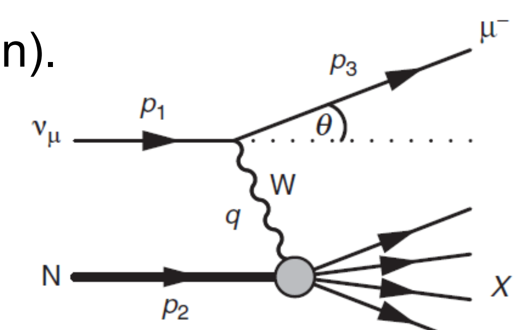

$$F_2^{\nu N} = x[u + \bar{u} + d + \bar{d}] \qquad xF_3^{\nu N} = x[(u + d) - (\bar{u} + \bar{d})]$$

$$F_2^{\nu N} = x[Q(x) + \bar{Q}(x)] \qquad xF_3^{\nu N} = x[Q(x) - \bar{Q}(x)]$$

Measurement: $F_2^{\nu N} + xF_3^{\nu N} = 2xQ(x)$ ➡ Sea and valence quarks

$F_2^{\nu N} - xF_3^{\nu N} = 2x\bar{Q}(x)$ ➡ Sea quarks

Neutrino iron (isoscalar target) scattering: *Phys.Rev.D74:012008,2006*

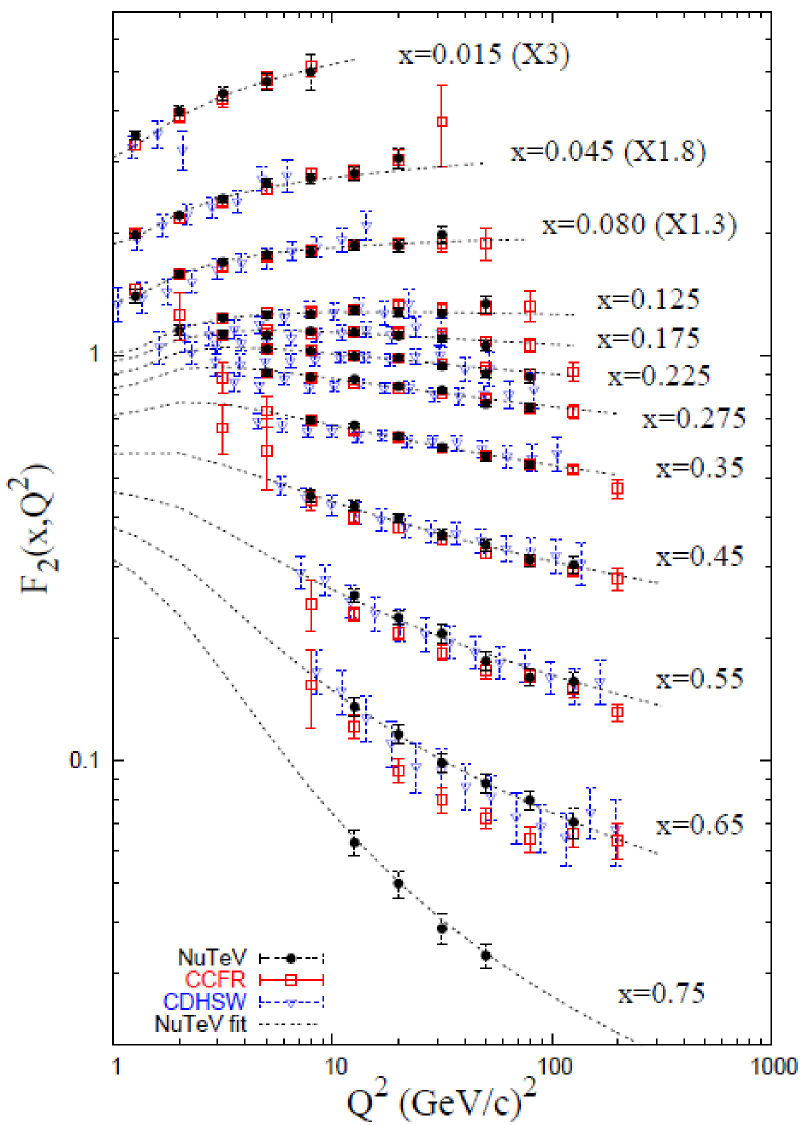

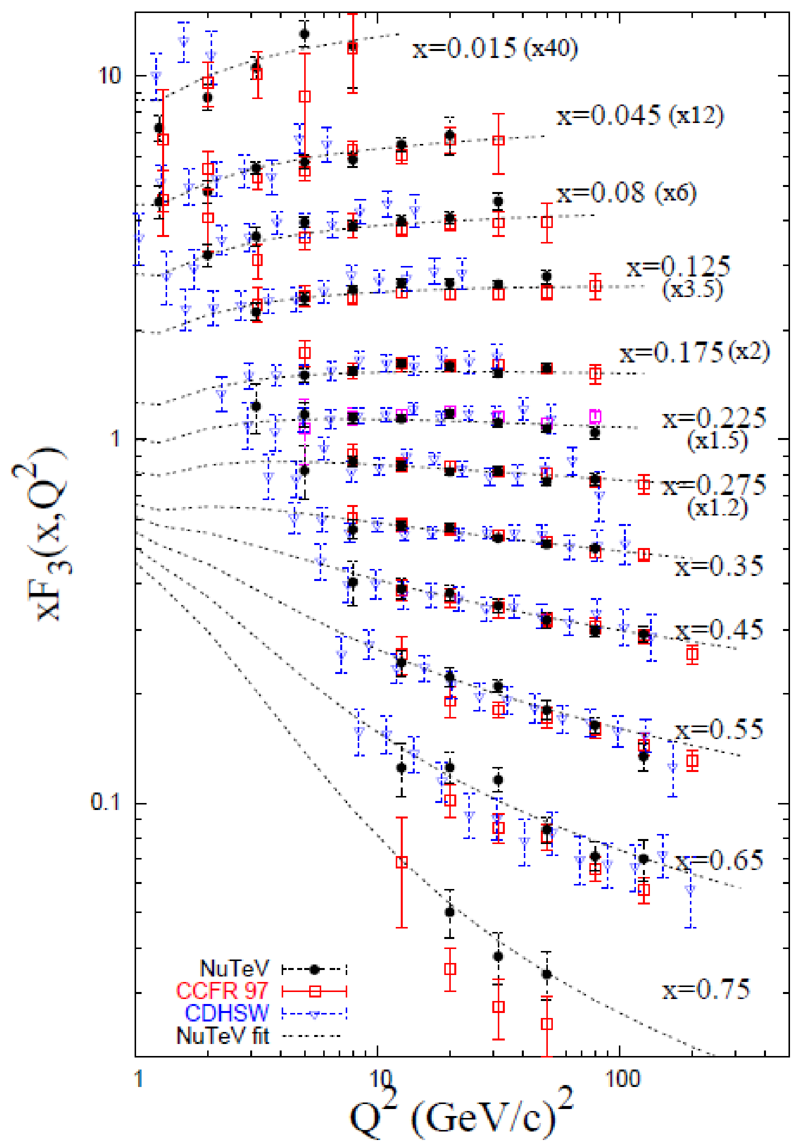

Determination of valence and sea quark distributions:

Taken from M. Thomson, based on *Phys.Rev.D74:012008,2006*

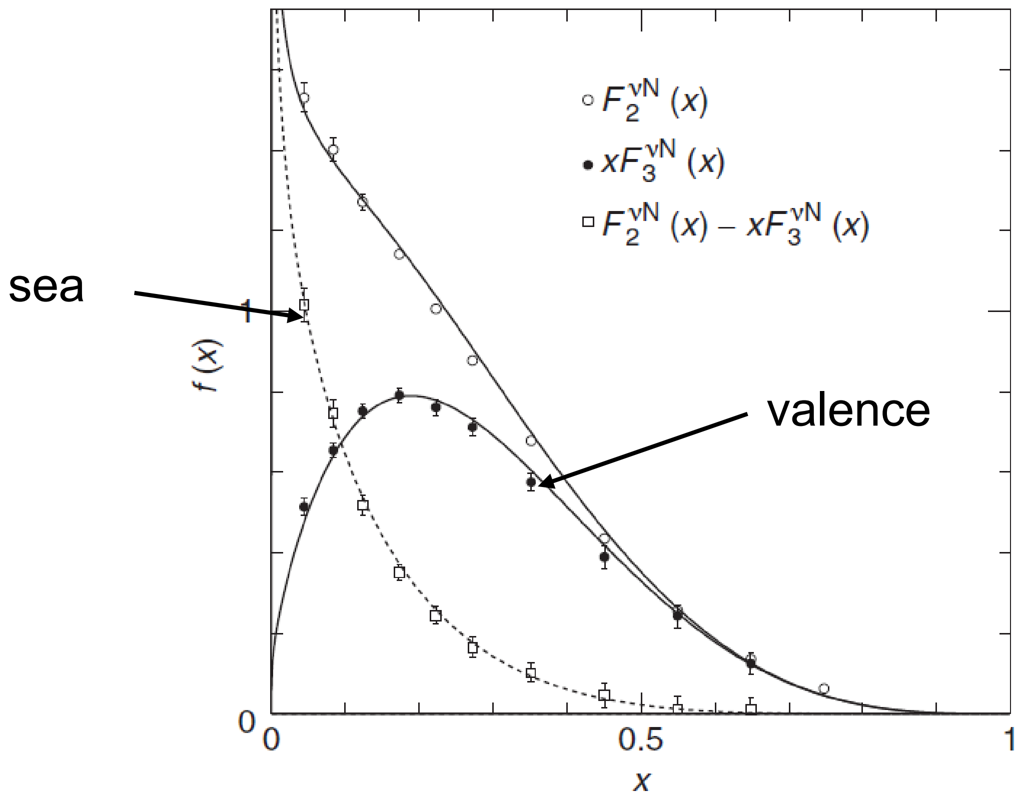

$$F_2^{\nu N} = x[Q(x) + \bar{Q}(x)]$$
$$xF_3^{\nu N} = x[Q(x) - \bar{Q}(x)]$$

Measurements of $F_2^{\nu N}(x)$ and $xF_3^{\nu N}(x)$ in neutrino/antineutrino nucleon deep inelastic scattering in the NuTeV experiment at Fermilab for 7.5 GeV^2 $< Q^2 <$ 13.0 GeV^2, compared to the expected distributions from the parton distribution functions at $Q^2 = 10$ GeV^2 shown in Figure 8.17. Data from Tzanov *et al.* (2006).

Recap: DGLAP and Scaling violation

"Symbolic"

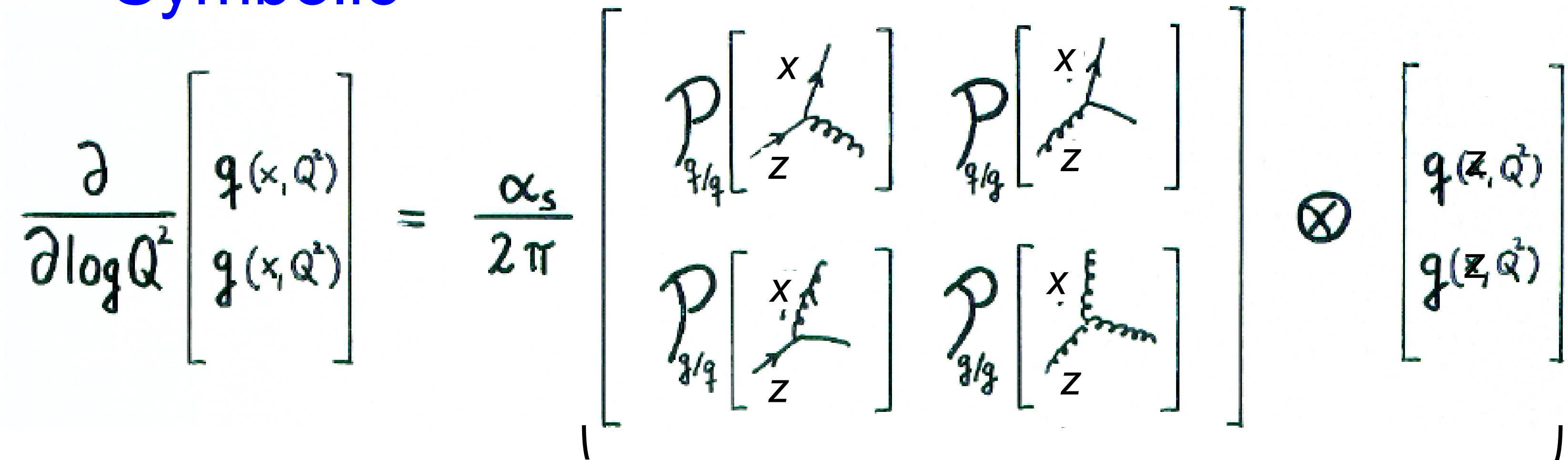

$$P \otimes f(x,Q^2) = \int_x^1 \frac{dz}{z} P\left(\frac{x}{z}\right) f(z,Q^2)$$

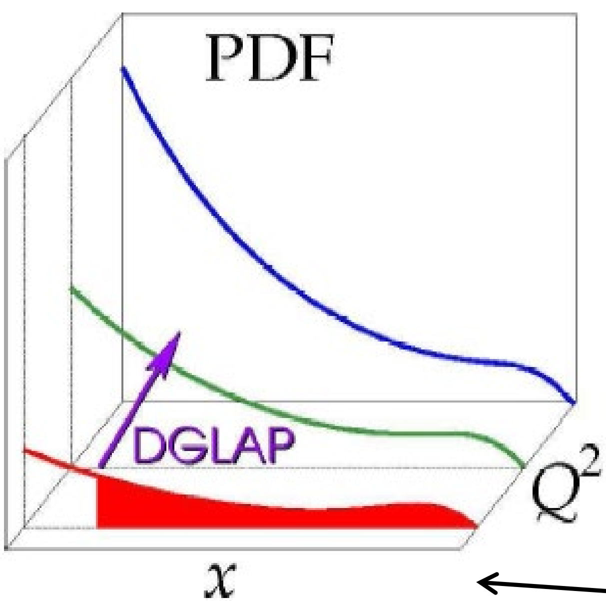

<u>QCD evolution:</u>

QCD predicts evolution of the PDF along the scale Q^2.

QCD cannot predict the shape of PDF, PDF must be measured!

Scaling violations for "pedestrians"

Large x: valence quark scattering

Small x: sea quark scattering

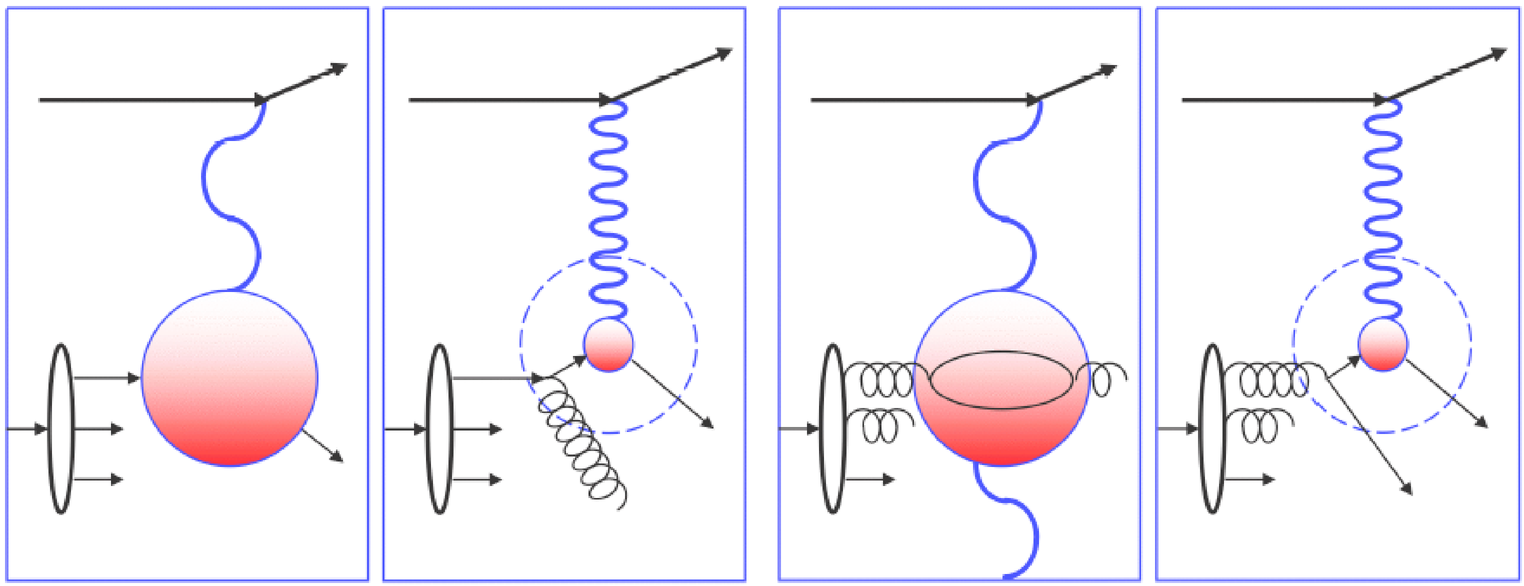

$Q^2 \uparrow \Rightarrow F_2 \downarrow$ for fixed (large) x

$Q^2 \uparrow \Rightarrow F_2 \uparrow$ for fixed (small) x

Scaling violation is one of the clearest manifestation of radiative effects predicted by QCD. PDFs depend on Q^2 (structure functions)

Measurement of PDFs at HERA

HERA

$e^{\pm}$ → 30 GeV

p ← 900 GeV

$$s = 4E_eE_p \approx 10^5\,\mathrm{GeV}^2$$

H1 detector

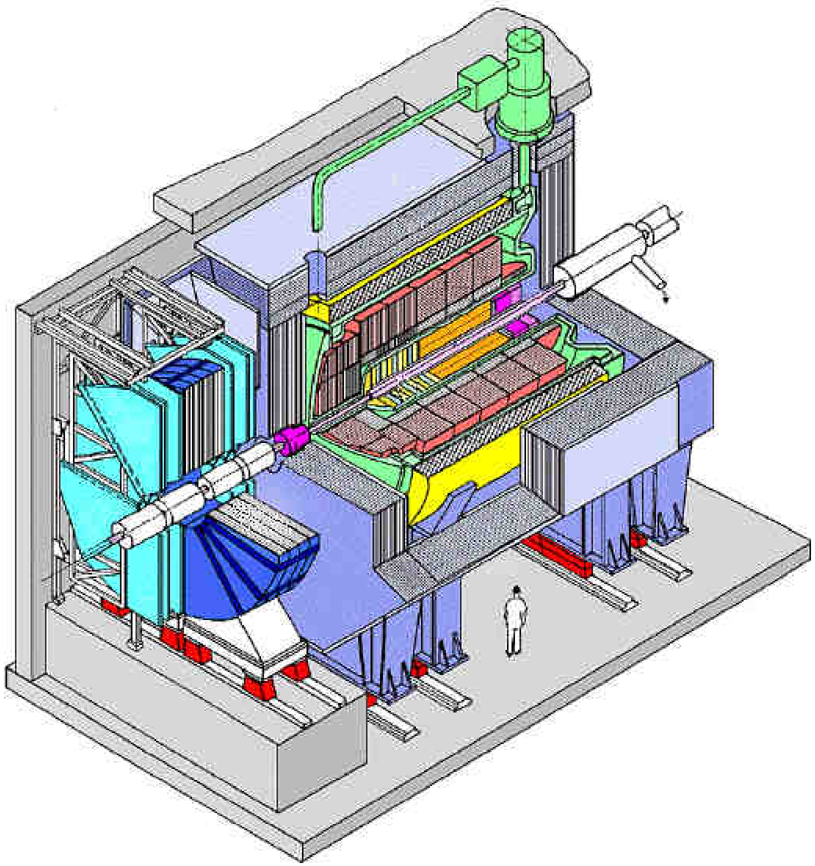

ZEUS detector

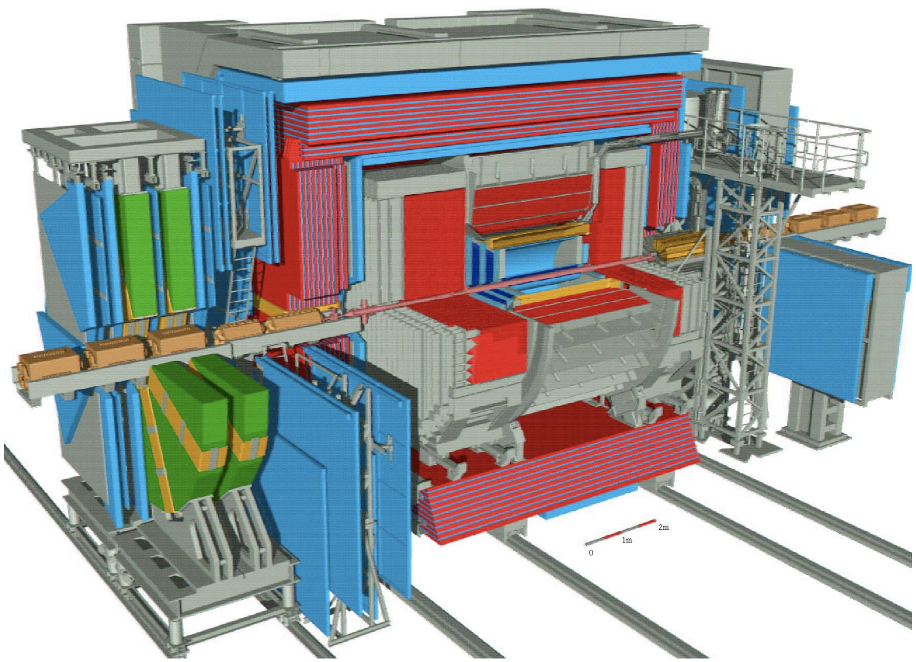

Q^2 = 25030 GeV^2, y = 0.56; **x=0.50**

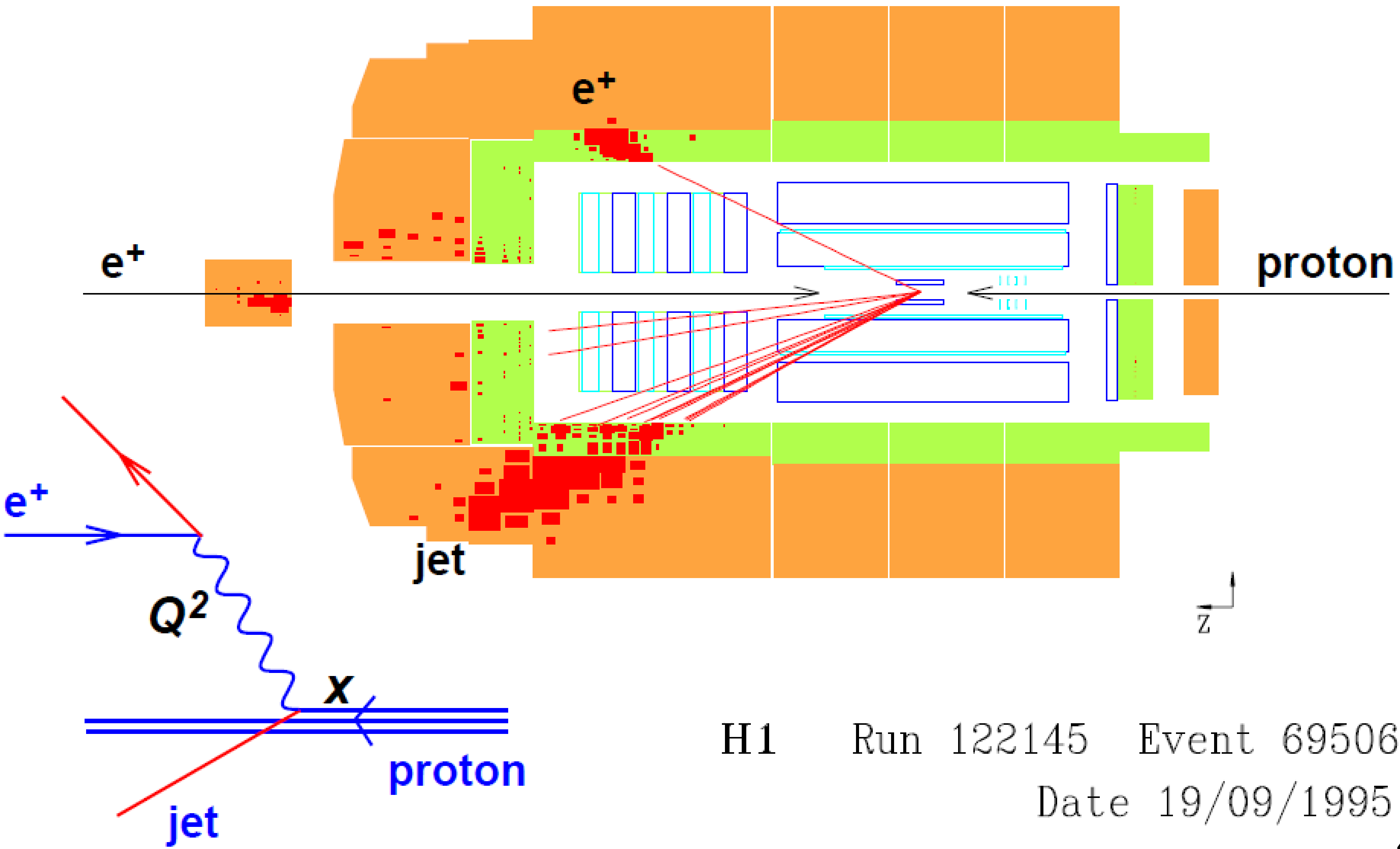

Accessible kinematic region

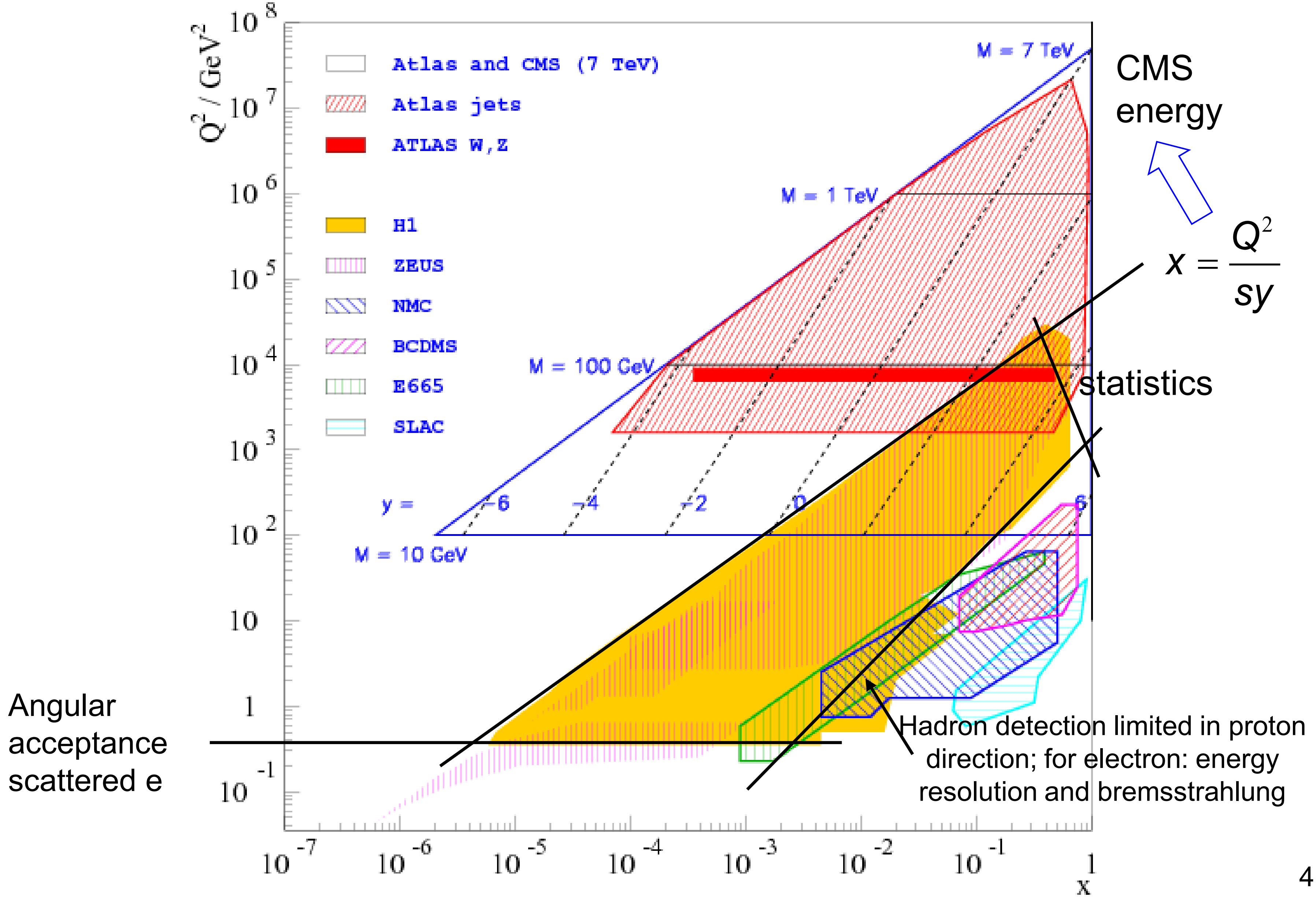

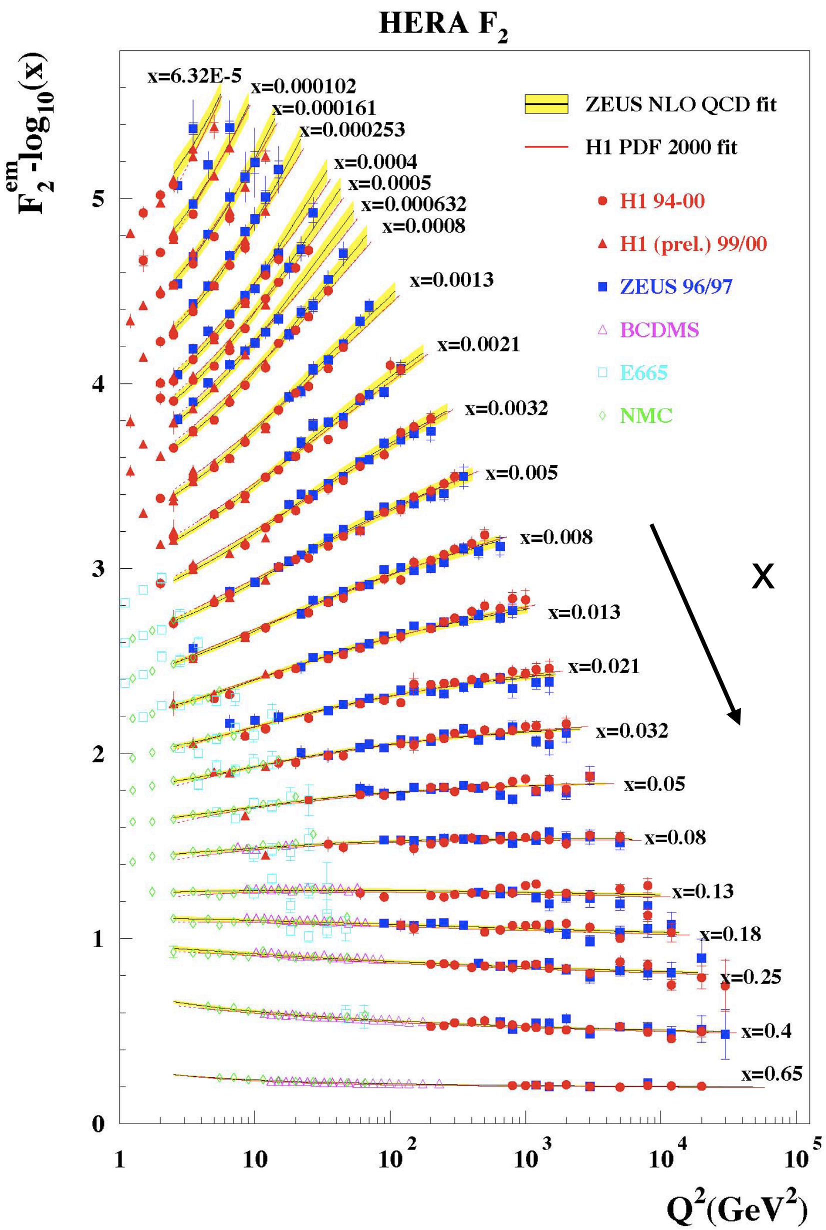

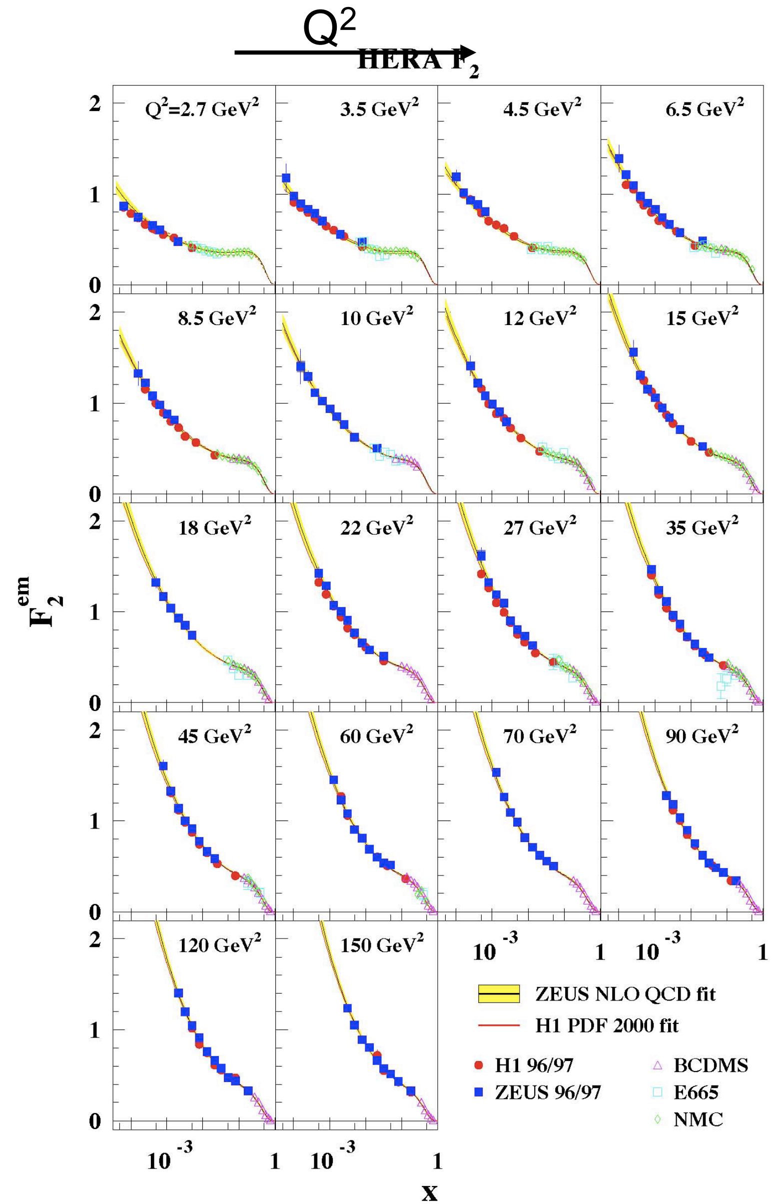

Determination of PDFs relies on factorization $d\sigma \sim d\sigma_{eq} \times F_2$

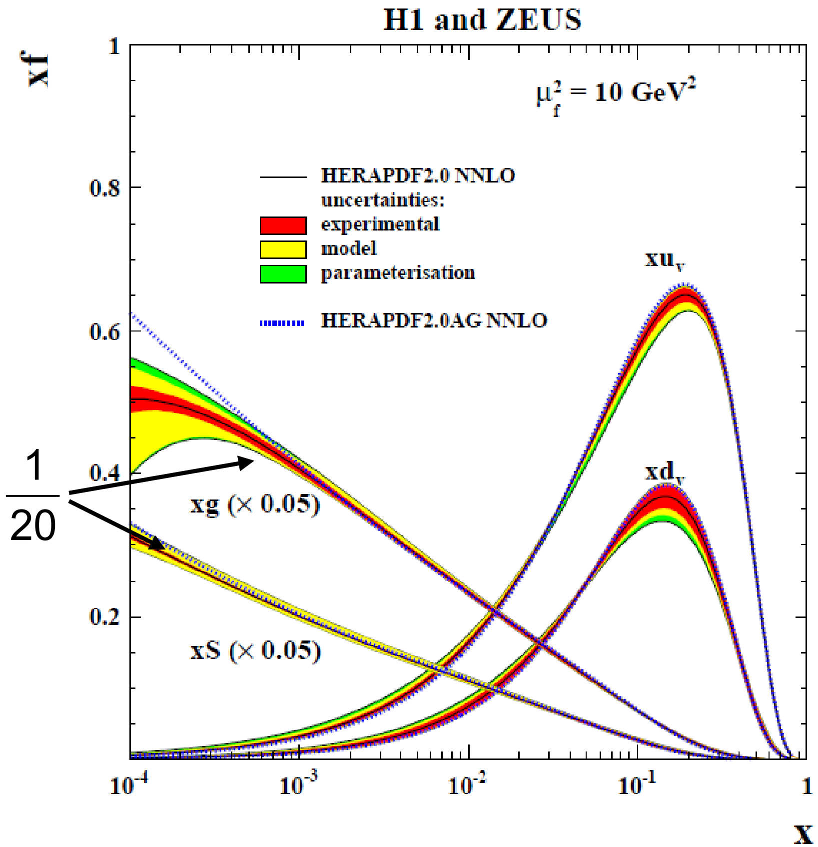

Figure 23: The parton distribution functions xu_v, xd_v, $xS = 2x(\bar{U}+\bar{D})$ and xg of HERAPDF2.0 NNLO at $\mu_f^2 = 10\,\mathrm{GeV}^2$. The gluon and sea distributions are scaled down by a factor 20. The experimental, model and parameterisation uncertainties are shown. The dotted lines represent HERAPDF2.0AG NNLO with the alternative gluon parameterisation, see Section 6.8.

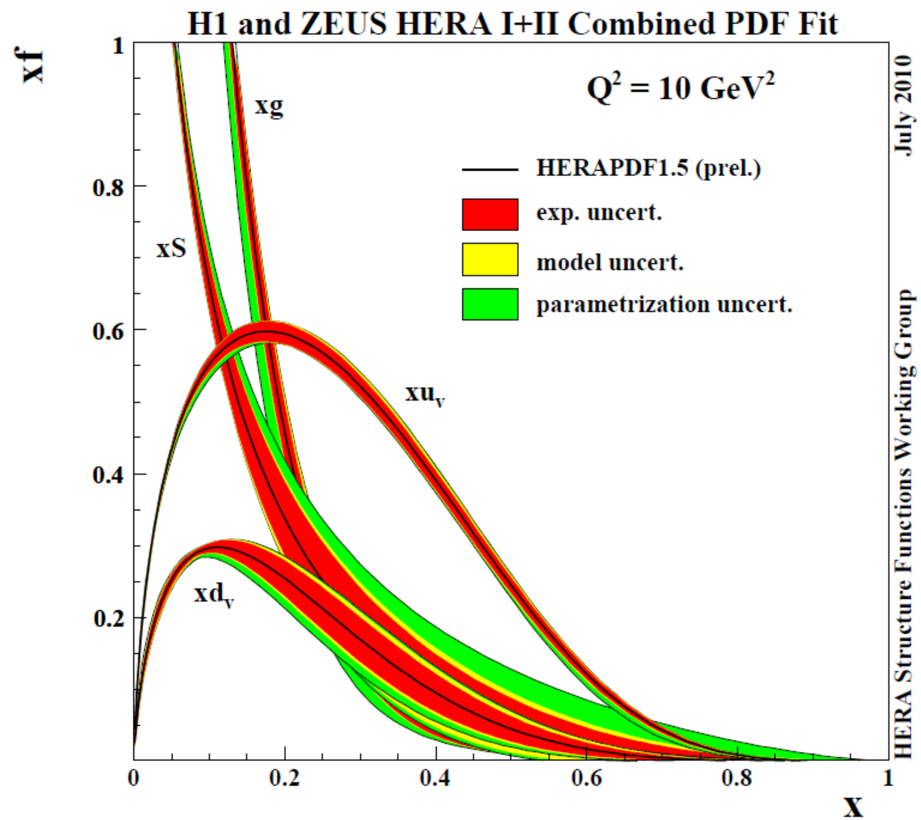

Linear scale for illustration (it is not exactly the same pdf set, but nearly)

Eur.Phys.J.C75 (2015) 12, 580

Q2 evolution

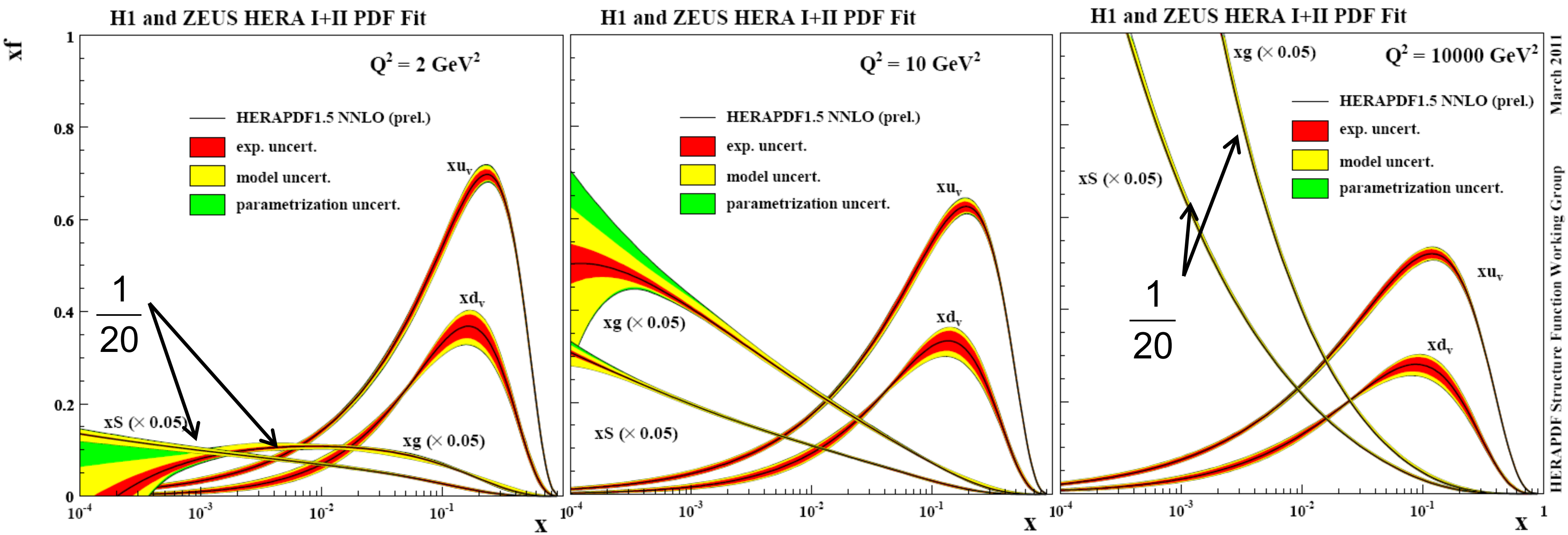

https://www.desy.de/h1zeus/combined_results/

The most dramtic of these [experimental consequences], that the protons viewed at ever higher resolution would appear more and more as field energy (soft glue), was only clearly verified at HERA ... F. Wilczek [Nobel Prize 2004]

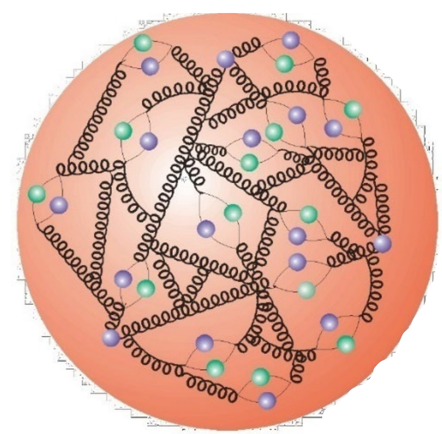

4. Hadron-hadron collisions

Factorization

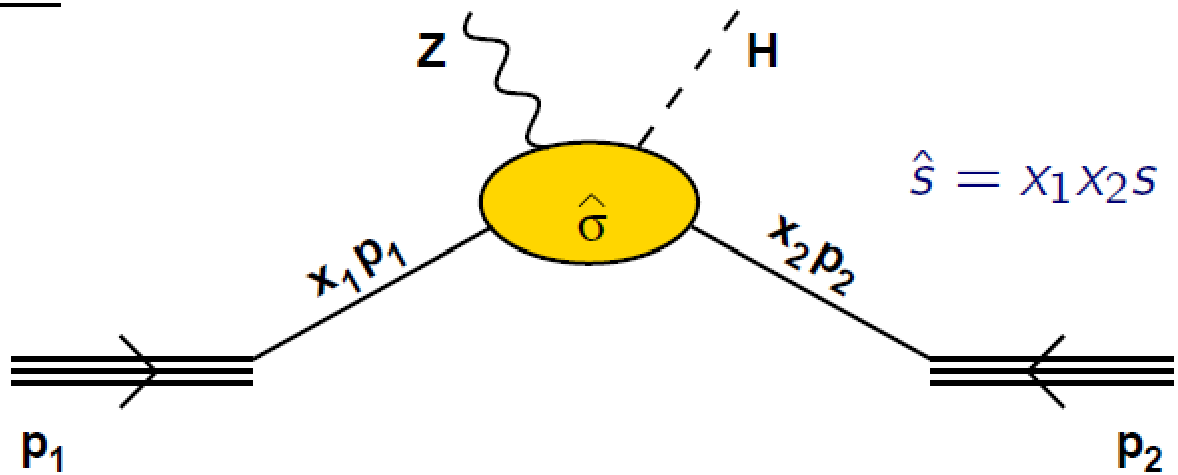

$\hat{s} = x_1 x_2 s$

$$\sigma = \int dx_1 f_{q/p}(x_1, \mu^2) \int dx_2 f_{\bar{q}/\bar{p}}(x_2, \mu^2)\, \hat{\sigma}(x_1 p_1, x_2 p_2, \mu^2)$$

factorization scale

Total cross section is factorized into a “hard part” and into a “normalization” from process independent parton distribution functions.

For all cross section estimation the knowledge of the PDF is necessary.